"Transition-Site" Model for the Permeation of Gases and Vapors through Compact Films of Polymers

PHILIP MOLYNEUX

Macrophile Associates, 53 Crestway, Roehampton, London SW15 5DB, United Kingdom

Received 27 October 1999; accepted 2 March 2000

ABSTRACT: The theory of the permeation of effectively spherical molecules of gases and vapors (permeants) through films of compact amorphous solids such as polymers is developed using the activated-jump model (AJM). The conventional view is that permeation has to be analyzed as the resultant of sorption (solution) and diffusion effects. By contrast, in the present article, it is proposed that permeation may be viewed as a simple or fundamental process. This is suggested by a number of experimental observations: (a) the permeation correlations of Stannett and Szwarc (1955–1956); (b) the "Permachor" concept of Salame (1961–1973); (c) the "ideal" permeation behavior of water vapor through moderately polar polymers; (d) the absence of any effect of oxidation on the water-vapor permeability of polyethylene (PE); and (e) the "isokinetic" correlations between the Arrhenius parameters for permeation. The conventional AJM for diffusion is analyzed using the principle of microscopic reversibility, which shows that the average jump is characterized by a "transition site" L at its midpoint, analogous to the transition state in chemical reactions. For amorphous solids, these transition sites would be structural features, distributed at random and with their axes pointing at random. This leads to the present transition-site model (TSM) of permeation, where, at the steady state, a certain fraction of these sites will be transiently occupied by molecules of the permeant in equilibrium with the free molecules at that level. The concentration of these free molecules corresponds to the thermodynamic activity at that point, that is, for gases and vapors, the partial pressure. The rate-determining step of the permeation process is then taken to be the release of the permeant molecule from the transition site according to classical transition-state theory. Using an idealized cubic-lattice model for the distribution of the transition sites, this is shown to lead to the observed proportionalities of the permeation rate to the area of the film, the pressure difference across it, and the reciprocal of the film thickness. It also accords with the observed Arrhenius-type dependence of the permeability coefficient on temperature, where the Arrhenius parameters relate to the thermodynamic parameters for the transfer of the permeant molecule from the gas phase and its insertion in the transition site. The Arrhenius parameters from the literature (*Polymer Handbook*) for 16 homopolymers—NR, PA 11, PC, PDMB, PDMS, three PEs (HDPE, LDPE, and hydrogenated polybutadiene), PETFE, PEMA, PET, PP, PTFE, PVAC, PVBZ, and PVC—with 16 "simple" permeants—H_2, He, CH_4, Ne, N_2, CO, O_2, HCl, Ar, CO_2, SO_2, Cl_2, Kr, SiF_4, Xe, and SF_6 as well as H_2O vapor—are used as the dataset. These Arrhenius parameters are first discussed in relation to isokinetic behavior. They are then correlated according to the TSM theory with the van der Waals molecular diameter of the permeant σ_G, and its absolute entropy S^0. With certain exceptions, linear correlations are obtained with the 10 smaller-molecule permeants (He to CH_4)

Correspondence to: P. Molyneux.

Journal of Applied Polymer Science, Vol. 79, 981–1024 (2001)

that show that they use the same set of transition sites, below and above the glass transition temperature, with each polymer; the permeant molecules evidently behave here as "hard spheres," regardless of their other chemical characteristics. This enables estimates to be made of the four characteristic parameters for the polymer: the intersite spacing λ (equivalent to the lattice parameter of the idealized model and to the jump length of the AJM); the size of the transition-site aperture, σ_L; the force constant θ associated with expansion of the aperture by the permeant molecule; and the entropy increment ν also associated with this expansion. For most of the systems, the site-spacing λ is of the order of 10 nm, and the aperture σ_L is about 200 pm. The theory provides a molecular basis for the interpretation and design of the permeation characteristics of polymers. J Appl Polym Sci 79: 981–1024, 2001

Key words: activated process; jump length; permeability coefficient; thermodynamics of permeation; transition-site model

INTRODUCTION

General Features of Permeation Through Polymers

The ability of solids such as polymers to transmit small-molecule substances has many practical applications and consequences, as well as being of great theoretical interest. This transmission involves the three interlinked processes of sorption (solution), diffusion, and permeation. In the case of polymers, permeation is important in a whole host of technical processes: dialysis, osmosis, reverse osmosis, pervaporation, ultrafiltration, and other membrane-separation processes; the dyeing of fibers and textiles; the behavior of barrier materials (balloons, geomembranes, gloves, packaging, tires, and so forth); the design of controlled drug-release systems; and the migration of plasticizers and other additives in polymers.[1–8]

In the present context, *permeation* refers to the process in which the *permeant* gas (or vapor) G passes through a layer (membrane, film, sheet, etc.) of the polymer (the *permeate*). This transmission from the bulk of the medium containing the permeant on one side of the layer to the bulk of the medium on the other side of the layer takes place under the influence of a difference in thermodynamic activity; this would be a pressure difference in the case of a gas or vapor or a concentration difference in the case of a solute in solution. Likewise, for volatile solids (camphor, disperse dyes, iodine, solid plasticizers, etc.), the driving force would be a difference in the vapor pressure of the solid.

With solids that are *porous*, the permeation involves the mass transport of the permeant. However, in the present article, we are concerned specifically with the behavior of solids that are *compact*, that is, that lack any well-defined pores, whether macroscopic or microscopic. The permeation must then involve the transport of individual molecules through the matrix of the solid. Of course, certain compact materials can acquire a porous structure by swelling when brought into contact with a solution of the permeant—this applies particularly to regenerated cellulose and hydrogels when brought into contact with the aqueous system involved.

Many polymers and related materials are semicrystalline, in that they contain both amorphous and polycrystalline regions, with the permeation taking place primarily through the amorphous region because of its "liquidlike" nature. Although in the present article we are concerned primarily with amorphous solids, the picture may be extended to the permeation behavior of composite materials, although there will be uncertainties of interpretation arising from ambiguities in differentiating between the amorphous and the crystalline regions in these materials.

The present treatment will also focus on permeants whose molecules are either inherently spherical (as with the monatomic noble gases) or which become effectively so by rotation (as with diatomic molecules and the simpler polyatomic molecules). For chain-molecule polyatomic permeants, reptation effects would come into play; the present treatment may cast some light on such reptation processes by providing a model for the behavior of the simpler spherical molecules.

Analysis of the Permeation Process

The process of permeation through a layer of a compact amorphous solid comprises a sequence of three stages:

(i) *Sorption* (dissolution) of the permeant at the surface layer of the solid in contact

with the phase of higher permeant activity;
(ii) *Diffusion* of the permeant molecules through the bulk of the solid to the other side of the layer under the influence of the concentration gradient across it;
(iii) *Desorption* (evaporation) of the permeant into the phase of lower permeant activity.

Some Definitions—Ideal and Nonideal Behavior

We may define *ideal permeation* as the simplest form observed experimentally, where the rate of permeation Q (the amount passing through the layer of sample in unit time) is given by

$$Q = -AP\Delta p/b \tag{1}$$

where A is the exposed area; Δp, the pressure difference; b, the thickness of the film; and P, the *permeability coefficient*. The negative sign in eq. (1) takes account of the flow being from high to low permeant activity, that is, in the opposite direction to the difference Δp. The proportionalities between Q and the area A, and the reciprocal thickness $1/b$, are almost invariably observed. Deviations are more often seen with the proportionality to Δp; such cases may be referred to as *nonideal permeation* and may be associated with the "plasticization" of the polymer by the sorbed permeant. For such systems, the value of P in the limit of very low pressures may be termed the *ideal permeability coefficient*, denoted by P_I:

$$P_I = \lim P(p \to 0) \tag{2}$$

The units used for the permeability coefficient P are discussed in Appendix A.

Likewise, in *ideal diffusion*, the rate of migration within the material is given by

$$Q = -AD\Delta c/b \tag{3}$$

where Δc is the concentration difference of the permeant across the bulk of the solid, and D, the diffusion coefficient. This is, of course, a statement of Fick's First Law of Diffusion. In this case, *nonideal diffusion* relates to systems where D is dependent on the value of Δc. For such systems, the value of D in the limit of very low concentration may be termed the *ideal diffusion coefficient*, denoted by D_I:

$$D_I = \lim D(c \to 0) \tag{4}$$

Likewise, *ideal sorption* may be defined by

$$c = Bp \tag{5}$$

where B is the sorption coefficient. This is also a statement of Henry's Law, so that B is one form of the Henry's Law coefficient for the system. *Nonideal sorption* is then characterized by the value of B being dependent on c (and p). The limiting value of B for low values of c (and p) may be termed the *ideal sorption coefficient* and is denoted by B_I:

$$B_I = \lim B(c \to 0) \tag{6}$$

Combining eqs. (1), (3), and (5) leads, for a triply ideal system, to the three coefficients being related by

$$P = BD \tag{7}$$

Likewise, for all systems, in the limit of low p and c, the relationship is that between the three ideal coefficients as specified earlier, that is:

$$P_I = B_I D_I \tag{8}$$

Restriction to Ideal Behavior

In the discussion that follows, unless otherwise specified, the permeation, diffusion, and sorption coefficients refer to the ideal values. The subscript "I" has accordingly been omitted from the symbols.

Temperature Dependence of the Coefficients

In considering the temperature dependence of these three coefficients, in the simplest cases, they all follow the same "exponential-reciprocal form." For permeation and diffusion, they follow the Arrhenius forms

$$P = P_A \exp(-E_P/RT) \tag{9}$$

and

$$D = D_A \exp(-E_D/RT) \tag{10}$$

where R is the gas constant; T, the absolute (thermodynamic) temperature; and E_P and E_D, the activation energies for the respective processes.

Likewise, the sorption coefficient follows the analogous van't Hoff form for equilibria:

$$B = B_V \exp(-\Delta H_S/RT) \quad (11)$$

where ΔH_S is the standard enthalpy change for the sorption process.

It is more customary, in these eqs. (9)–(11), to use a subscript zero with the preexponential factors, but in the present case, the subscript "A" (Arrhenius) or "V" (van't Hoff) is used to differentiate these from the ideal values in eqs. (2), (4), and (6), which are commonly likewise characterized by a subscript zero. This also reminds us that these preexponential factors are the values in the hypothetical limit of very high (infinite) temperature, rather than of very low (zero) absolute temperature as a subscript zero would suggest.

It should be noted that eq. (11) has a thermodynamic basis, in that, in principle, the value of the enthalpy change could be determined directly by calorimetry and should agree with that from the van't Hoff eq. (11). By contrast, the activation energies E_P and E_D are derived solely from eqs. (9) and (10).

Comparing the temperature-independent and temperature-dependent parts of eqs. (9)–(11) in the light of eq. (8) gives

$$P_A = D_A B_V \quad (12)$$

$$E_P = E_D + \Delta H_S \quad (13)$$

Effects from the Glass Transition and Melting Points

One complicating effect here is that frequently the Arrhenius plot shows a break at the glass transition temperature, T_g, indicating that the "glass" state ($T < T_g$) and the "rubber" state ($T > T_g$) have different values of the Arrhenius parameters and, hence, presumably show different behavior at the molecular level. This is discussed later in the article. This situation means that, strictly speaking, the parameters should be labeled with the state that is involved.

Likewise, breaks may be expected if the melting temperature is within the experimental temperature range, although this is less commonly encountered in practice.

Even for a purely amorphous polymer at temperatures away from the T_g, deviations may be expected from the simple equations above if the temperature range is wide enough—even in the absence of glass transition or melting effects, a polymer at 100°C is a different material from that at 0°C; however, such effects are not generally encountered because the temperature ranges used are much narrower than this.

PERMEATION VIEWED AS A "PRIMARY" PROCESS

The foregoing analysis of permeation into the three successive steps (sorption, diffusion, and desorption) is long-established, while the derivation of eq. (7) and the establishment of the Arrhenius behavior is only somewhat less mature.[9–17] The entrenched character of this overall picture has led to the firmly held assumption that, according to eq. (7), permeation is a secondary process—to be interpreted as a composite of sorption and diffusion as two primary processes. Evidently, even from a purely practical viewpoint, this is a hindrance in (say) the design of a barrier material, since it means that the sorption and diffusion characteristics must be separately designed in, but, at the same time, balanced in such a way that the correct permeation characteristics are obtained.

However, there are a number of instances in the published literature where the permeation behavior is simpler than might be expected with the above picture and in such a way as to suggest that permeation may be a primary or fundamental process. We cite five examples here:

Stannett–Szwarc Correlation

More than 40 years ago, Stannett, Szwarc, and their coworkers pointed out that, although the permeation coefficient for a particular gas in a range of polymers may vary over many orders of magnitude, the ratio of the permeability coefficients for a pair of gases can be almost constant.[18,19] They used the permeant gases N_2, O_2, CO_2, and H_2S (at 30°C), with a dataset of 22 polymers ranging from low permeability ones such as Mylar (PET) to highly permeable ones such as the elastomers natural rubber (NR) and polyisobutene (PIB) (Table I). Although the P values ranged over three orders of magnitude, nevertheless, the mean value of the ratio $P(O_2)/P(N_2)$ was 3.8(8), while for $P(CO_2)/P(N_2)$, it was 24(7),

Table I List of Polymers for the Stannett–Szwarc Correlation

Polymer			
Code	Designation	Details	$17 + \log F_M$
A	Buna S	Poly(Bu-*co*-S)	4.678
B	Butyl rubber	Polyisobutene	3.369
C	Cellulose acetate (plasticized)	—	3.574
D	Cellulose acetate P-912	—	3.322
E	Ethyl cellulose (plasticized)	—	4.799
F	Hycar OR 15	Poly(An-*co*-Bu): 39:61	3.246
G	Hycar OR 25	Poly(An-*co*-Bu): 32:68	3.656
H	Kel F (Trithene)	Polychlorotrifluoroethylene	2.989
I	Methyl rubber	Polydimethylbutadiene	3.556
J	Mylar	Poly(ethylene terephthalate)	1.574
K	Natural rubber	*cis*-Poly(isoprene) (NR)	4.782
L	Neoprene	Polychloroprene	3.947
M	Nylon 6	Polyhexanoamide	1.875
N	Perbunan	Poly(An-*co*-Bu): 27:73	3.900
O	Pliofilm FM	NR hydrochloride	3.021
P	Pliofilm NO	NR hydrochloride	1.778
Q	Pliofilm P4	NR hydrochloride	3.667
R	Polybutadiene	—	4.685
S	Polyethylene	—	4.154
T	Poly(vinyl butyral)	—	3.273
U	Saran	Poly(vinylidene chloride)	0.848
V	Vulcaprene	Polyurethane	3.565

Code: letter codes for the polymers in Figure 1. Designation: names used in the original articles.[18,19] Details: from the literature (An = acrylonitrile, Bu = butadiene, S = styrene).[6] F_M: factor for the polymer in the Stannett–Szwarc correlation at 30°C (303 K), equal by definition to the permeability coefficient for N_2.

and for $P(H_2S)/P(N_2)$, it was 22(7) (Fig. 1).* This enabled them to assign multiplicative numerical factors to the individual gases and polymers, using an equation of the form

$$P = F_M F_G F_{GM} \tag{14}$$

where F_M is the factor for the polymer; F_G, that for the permeant gas; and F_{GM}, that accounting for any specific interaction effects between the two (in the original articles, these three factors were designated F, G, and γ). The derived values of F_M, using $F_G = 1$ for N_2 and assuming that $F_{GM} = 1$, are listed in Table I.

This correlation was noted in a chemical engineering text[4] and in a polymer chemistry text.[8] However, the lack of a theoretically justifiable explanation, coupled with the belief that permeation must be composite, has evidently inhibited its use even as an empirical correlation.

The "Permachor" Concept of Salame et al.

A parallel approach to correlations for the permeability coefficient was that of Salame et al. who introduced the concept of "Permachor" π_S as an additive property related to the molecular structure of the polymer and/or the permeant.[20–23] In the early publications,[20,21] attention was focused on the permeation of liquids through a single type of polyethylene (PE). The logarithm of the permeability coefficient was related to the sum of the Permachor values of individual groups (or atoms) in the permeant molecule

$$\log P = K_S - 0.22\pi_S(G) \tag{15}$$

with

$$\pi_S(G) = \sum \pi_S(\text{groups}) \tag{16}$$

* See the Nomenclature section at the end of this article for the method of representing mean and standard deviation values.

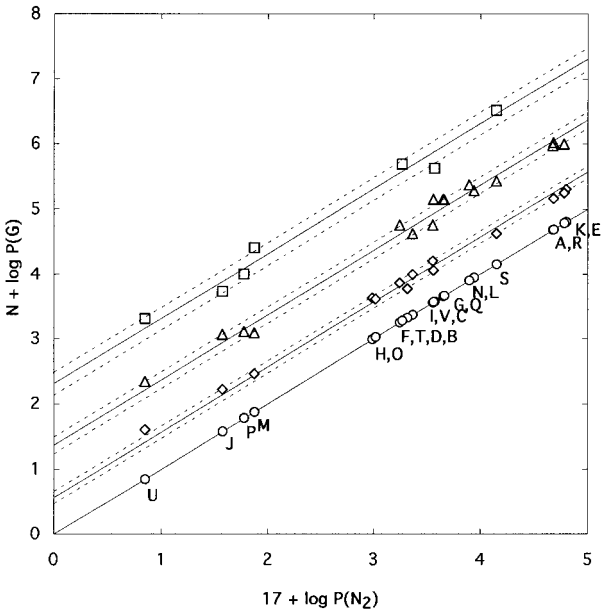

Figure 1 Stannett–Szwarc correlation: log–log plot of the permeability coefficient P (in "standard" units—Appendix A) for the permeant G versus that for N_2 at 30°C (303 K); see Table I for the polymer codes. Permeant symbols (with value for the ordinate scaling factor N): (○) N_2 (N = 17—reference line); (◇) O_2 (N = 17); (△) CO_2 (N = 17); (□) H_2S (N = 18). Data from refs. 18 and 19.

where the "Salame constant" K_S is a parameter that depended only on the temperature. This was extended to other types of PE, and to polypropylene (PP), with different values for the parameter K_S.

From the present viewpoint, the permeation coefficients for these liquids would need to be corrected appropriately if they are to be compared with the data for gases and vapors, by introducing the vapor pressure of the liquid. At the same time, these might not be expected to be the ideal values P_I because of possible "plasticization" of the polymers (to different extents) by the different liquids.

In later work on permeation of gases (O_2, N_2, CO_2) through a wide range of polymers, the Permachor concept was applied to the polymers, using contributions from the structural groups of the polymer chain.[22] It is interesting that these particular data were found to follow the Stannett–Szwarc-type behavior (see above), in that for the 84 polymers listed and a temperature of 25°C the value of the ratio $P(O_2)/P(N_2)$ was 4.0(23) and that of $P(CO_2)/P(O_2)$ was 3.6(20). This appears to be have been noted independently of the Stannett–Szwarc work.[18,19]

The same concept was subsequently applied to the permeation of gases and water vapor though the acrylonitrile copolymer "barrier resins."[23]

These correlations by Salame were noted in a chemical engineering text,[4] but not apparently in the main polymer literature; presumably, they have been considered as purely "empirical" correlations, lacking any fundamental significance because of the presumed composite nature of the permeability coefficient value.

Permeation of Water Vapor Through Polymers

In general, a polymer/permeant system follows one of two forms of behavior, that is: (a) It is triply ideal in that all three eqs. (1), (3), and (5) are obeyed or (b) it is triply nonideal, in that all three coefficients show dependence on the pressure and concentration levels of the permeant.

In the case of water as the permeant, behavior (a) applies to nonpolar polymers such as (pure) PE, and behavior (b), to highly polar polymers such as poly(vinyl alcohol), nylon, and regenerated cellulose.[24,25]

However, as the present author noted,[25] an interesting intermediate situation applies in the case of water vapor with moderately polar polymers, in that the permeation behavior is ideal although both sorption and diffusion are nonideal. This is applies to silicone rubbers,[26,27] poly(alkyl methacrylate)s,[28,29] natural and synthetic rubbers,[30] (oxidized) PE,[31,32] poly(vinyl butyral),[33] poly(vinylidene chloride-*co*-acrylonitrile),[33] natural rubber hydrochloride,[34,35] cellulose acetate,[33] and ethyl cellulose.[35–37] However, the behavior with polyoxymethylene and poly(vinyl chloride) is less clear-cut.[38]

In this context, water might be thought not to be a suitable example, since its behavior is well known to be anomalous. However, this applies primarily to water in the liquid state, whereas in permeation through compact polymers, we are concerned with isolated water molecules in the polymer or, at most, clusters of small size.[24]

Again, this "simple" permeation behavior has evidently not been considered to be significant, but, rather, presumed to be the result of a coincidental cancellation of the deviations from ideality of the sorption and diffusion processes.

Permeation of Water Vapor Through Oxidized PE

With the above-cited early studies by Rouse on PE, the water sorption was high in comparison

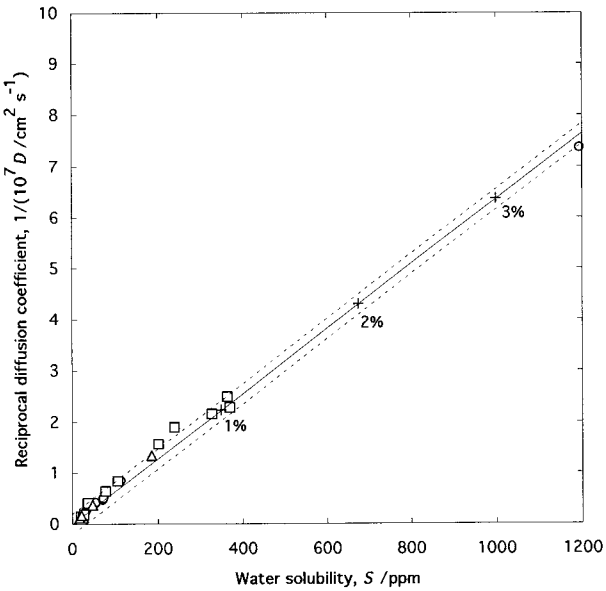

Figure 2 Reciprocal diffusion coefficient, D^{-1}, versus liquid solubility S at 298 K (25°C) for H_2O with three samples (Specimens B, C, and D) of PEs after oxidation. Key: (○), Specimen B; (□), specimen C; (△), specimen D; + (and running numbers), combined oxygen content in percent. The straight line through the origin corresponds to permeability coefficient $P = 5.4(11) \times 10^{-12}$ "standard" units (Appendix A) for H_2O/PE. Data of McCall et al.[31]

with that from other studies, evidently arising from the oxidation of the polymer in processing.[32] Subsequently, McCall and coworkers[31] studied the permeation of water vapor (from the pure liquid) through three specimens of oxidized PE. These had been oxidized to controlled extents (by milling in the air in the absence of any antioxidant) to give combined oxygen contents up to about 3%. They found that, although this naturally enhanced the sorption coefficient (up to 50-fold) compared with the starting polymer, the diffusion coefficients suffered compensating reductions, so that the permeability coefficient was essentially unchanged by this treatment (Fig. 2). Here, again, this "simple" permeation behavior has been considered as accidental, that is, the by-product of coincidental canceling of sorption and diffusion effects.[31]

Correlations Between the Arrhenius Parameters for Permeation

When the Arrhenius parameters for permeation for ranges of polymers and permeants are examined, it is frequently found that there is an essentially linear correlation between $\log P_A$ and E_P for various permeants with the same polymer; this is discussed with specific examples later in the article. This type of "isokinetic" relationship again suggests that permeation may be viewed as a primary process, although, similarly, it may be ascribed as the result of such relationships applying to both the component processes of sorption and diffusion.

THE ACTIVATED-JUMP MODEL OF DIFFUSION

Before developing the present transition-site model (TSM), which is the main theme of this article, it is necessary to outline the "activated-jump" model (AJM) which has been used widely for modeling diffusion in solids including polymers.[39–48] This outline serves both to point out the features of the model widely accepted at present and to show how a closer examination of these features leads to the concept of the transition site.

In the AJM, the sorbed molecules of the permeant are assumed (implicitly or explicitly) to occupy definite equilibrium positions in the matrix of the solid. The molecule is then assumed to migrate between two such adjacent positions by a thermally activated jump; a lattice picture for this is shown in the upper part of Figure 3. The main evidence for this jumping is the Arrhenius form of eq. (10) for the temperature dependence of the diffusion coefficient. The observed diffusion then involves a sequence of such jumps in a biased random flight, with the net movement taking place down the concentration gradient; this arises simply because, for two such adjacent sorption locations, the greater number of sorbed permeant molecules at the "upstream" location leads to a greater number of jumps in the "downstream" direction.

The activation energy E_D in eq. (10) is then identified with the extra energy (above its normal thermal energy) that the molecule must acquire for it to be able to perform its jump. With the simplest picture, this energy is accumulated by random fluctuations in the thermal energy at the location of the sorbed molecule, with a probability given by the Boltzmann factor: $\exp(-E_D/RT)$. A more complex picture is the "zone theory," where the energy is taken to be accumulated from many

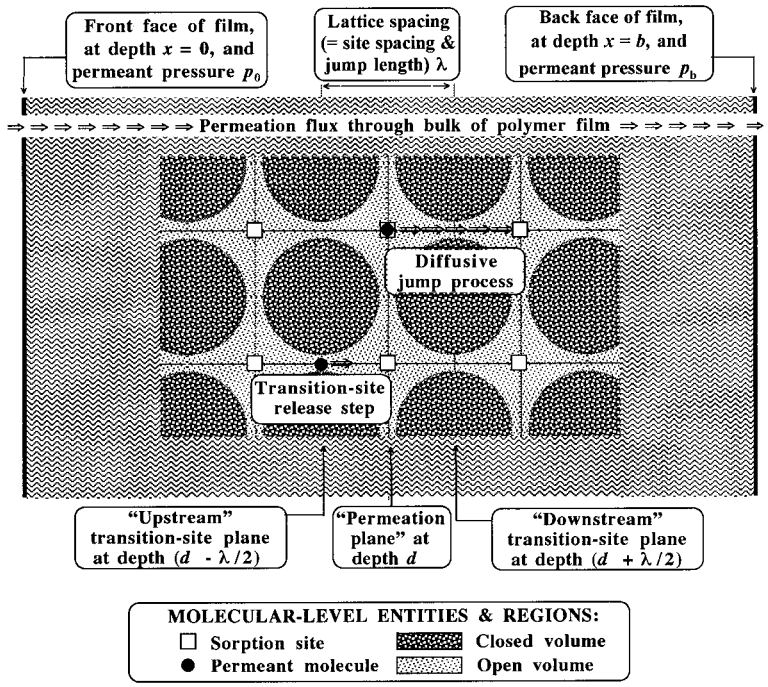

Figure 3 Diagram for permeation through a polymer film of thickness b. The permeation takes place in the direction of the x-axis. The sample has a permeant pressure p_0 on the front face ($x = 0$) and a pressure p_b on the back face ($x = b$). The center of the diagram represents a cubic lattice, with lattice parameter (= intersite-spacing = diffusive jump length) λ. The "closed volume" is shown as heavily shaded areas, and the "open volume," as the lighter-shaded remaining area. Open squares (□) represent the preferred (lowest free energy) sites for sorption; filled circles (●) represent molecules of the permeant G. The upper part of the diagram illustrates the AJM for diffusion, showing the process of the activated jump from one sorption site to the next one, through the permeation barrier (transition site). The lower part of the diagram illustrates the present TSM for permeation, showing the release of a molecule of G from the transition site L.

degrees of freedom of the thermal energy in the surrounding matrix.[13,14]

To analyze this further, we may apply the Principle of Microscopic Reversibility (PMR); in the chemical context, this is referred to as the Principle of Detailed Balancing. The PMR requires that, for any molecular process, the forward and reverse forms of that process have the same probability.[49] In the present context, this requires that if we reverse the sequence of events in the jump process this gives an equally probable form of jump, so that the (average) jump must be symmetrical about its midpoint. In particular, the behavior in the second part of the jump must mirror that in the first part; the permeant molecule must arrive at its final location with the same energy with which it started out, and this energy must be dissipated into the matrix of the polymer in a fashion mirroring that by which it was acquired at the start of the jump.

If we analyze the activation energy for diffusion, E_D, then this is composed, in part, of the energy to free the molecule from its sorption site, and if the molecule is then taken to be completely free at the start of the jump, then the energy required will be the enthalpy change for *desorption*, $-\Delta H_S$. Thus, by eq. (13), the energy left will be the permeation activation energy, E_P. Thus, one feature of permeation makes its appearance even at this early stage of the analysis.

The fact that the molecule has to be "activated" in this way shows that it needs to overcome a resistance to its motion in its jump, which slows it down over the early part of its jump, while by the PMR it will be speeded up progressively over the later part. To make the process symmetrical as required by the PMR, the "early part" will be the first half and the "later part" will be the second half of the jump, with the velocity being a minimum at the midpoint of the jump. Now because of

the exponential dependence of the Boltzmann factor on the energy term, this energy must be the absolute minimum that is required if the jump is to be successful, and the midpoint velocity must likewise be the absolute minimum.

The PMR does not seem to have been used previously, at least explicitly, as a criterion in choosing acceptable mechanisms for diffusion and permeation. It should be noted, in particular, that any (average) jump sequence that is proposed must be symmetrical; any unsymmetrical process—for example, a permeant molecule jumping into a hole formed in its neighborhood—is not acceptable.

TSM FOR PERMEATION

Basis of the Model

In this model, we focus our attention on the behavior of the midpoint of the activated jump already discussed. In the transition-state theory of chemical reactions, the reactants are required to pass through a transition state before they can form the products.[50,51] By analogy, this midpoint is referred to here as the "transition site," whose locations are symbolized by L. Following the framework of the AJM, where the sorption sites must be taken to be fixed, the transition sites must likewise be taken to be at fixed positions in the polymer matrix. The transition state in chemical reactions is the point of maximum (free) energy on the path along the "reaction coordinate" from the reactants to the products, while in this state the (free) energy is locally a minimum in all directions at right angles to the reaction coordinate. Likewise, in the transition site L, the permeant molecule has maximum (free) energy in the direction along the axis of the site (which is the direction of the jump) and a minimum in all directions at right angles to this axis.

Lattice Model

With an isotropic amorphous material such as a polymer, the transition sites L will be distributed at random in the matrix, with their axes likewise directed at random. Such a picture is difficult to deal with mathematically. For tractability, therefore, we will work with an idealized lattice model, whose consequences should still apply to the real situation.

We therefore use a simple cubic-lattice model, as shown in Figure 3. The lattice cube is viewed as having a central cavity for the sorption of the permeant, communicating with the adjacent cavities by way of the transition sites L on the faces of the cubes that represent restrictions or "bottlenecks."[25] The "closed volume" (that not accessible to G) is that represented in Figure 3 by the dark-shaded circles, while the "open volume" (that accessible to G) is the lighter shaded parts of the diagram. The transition sites that connect these latter parts would be radially symmetrical about their axes.

The jump length is then the lattice spacing, symbolized here by λ. In the later application of the model, when we have to revert to a nonlattice "random" picture, the parameter λ becomes simply the average intersite spacing, albeit still equivalent to the jump length of the AJM.

For further simplicity, the lattice is taken to be aligned with the surface of the sheet (of area A) in the yz-plane so that the permeation takes place along the x-axis of the system; here, the x-value will run from zero at the front face to the thickness b at the back of the sheet. The transition sites then divide into three types by the direction of the axis, that is, L_x, L_y, and L_z. By this means, only the transition sites of type L_x will contribute to the permeation process that is taking place along the x-axis.

The permeation will be taken to be ideal, so that the value of the permeability coefficient is the same throughout the layer. The permeant molecules will be taken to be either spherical (i.e., the noble gases) or to be effectively so at these temperatures by reason of their rotation. This should therefore apply to diatomic molecules such as N_2, H_2, and O_2 and even to simple polyatomic molecules such as CH_4, CO_2, and H_2O.

Permeant Insertion Equilibrium at the Transition Sites

Considering Figure 3, for the permeant G at (partial) pressure p_0 on the front of the sheet ($x = 0$) and p_b on the back ($x = b$) the pressure difference across the sheet is

$$\Delta p = p_b - p_0 \tag{17}$$

With a steady-state flux of permeation, there will be a linear gradient of permeant pressure within the sheet. This may be visualized (and could be realized) as the pressure that would be set up in a

small (microscopic) cavity at that point; alternatively, it would be the pressure set up if the sheet were sliced across in the yz-plane at this level, the two parts slightly separated, and the steady state resumed. This gradient was constructed mathematically for the system (oxidized) PE/water by Rouse.[32] In more general terms, it is the gradient of thermodynamic activity of the permeant, whose significance in these processes was discussed by Kuppers and Reid[52] and by Reiss.[53]

Thus, at the level at general distance x from the starting plane, the partial pressure p_x is given by

$$p_x = p_0 + x\Delta p/b \tag{18}$$

For a particular transition site L, the insertion process of its occupation by a molecule of permeant G will be controlled by the equilibrium

$$G(x) + L(x) \rightleftharpoons GL(x) \tag{19}$$

where the depth is specified because the partial pressure of G will depend on this.

The equilibrium of eq. (19) will be governed by an equilibrium constant $K^{\ddagger}$ (using the superscript double dagger "‡," which is the conventional symbol for the transition state) whose value will be characteristic of the system. It will relate the equilibrium concentrations of the three species at each particular level according to

$$K^{\ddagger} = [GL(x)]/[G(x)][L(x)] \tag{20}$$

where $[G(x)]$ is the partial pressure of the permeant; $[L(x)]$, the concentration of unoccupied transition sites L; and $[GL(x)]$, the concentration of occupied transition sites, all at the depth x. Note that this assumes that the system can be characterized by a unique value of $K^{\ddagger}$, whereas because of the amorphous character of the material it is likely that there is a distribution of values. However, the distribution cannot be too broad; otherwise, we would not get the observed Arrhenius form for the temperature dependence of P.

Evaluation of the Rate of Permeation

To calculate the rate of permeation for this model, as shown in Figure 3, we chose as the "plane of permeation" that at depth d that passes through the center of the cubes. This has a plane of transition sites L (partially occupied by the permeant) at distance $\lambda/2$ on either side. This choice of the plane of permeation ensures that the molecules released from the transition sites on either side reach it at the same time. At the corresponding levels of these transition sites L, the partial pressure of the permeant will be given, following eq. (18), by

$$[G_{\pm}] = p_0 + (d \pm \lambda/2)\Delta p/b \tag{21}$$

where the positive and negative signs, respectively, denote the "downstream" $(d + \lambda/2)$ and "upstream" $(d - \lambda/2)$ sides of the central plane.

Since with ideal permeation the degree of occupancy of the transition sites L is (vanishingly) small, by putting these in terms of the number of sites exposed over the area considered (A), the ratio of the number of sites occupied, n, to the total number of sites, n_{tot}, will be given by

$$n/n_{tot} = [GL]/[L] \tag{22}$$

The total number exposed over this area will be

$$n_{tot} = A/\lambda^2 \tag{23}$$

since each transition site is at the center of a square of edge λ (Fig. 3), so that combining eqs. (20)–(23) gives

$$n_{\pm} = (A/\lambda^2)K^{\ddagger}[p_0 + (d \pm \lambda/2)\Delta p/b] \tag{24}$$

We can now apply the standard transition-state theory[50,51] to obtain the rates at which the permeant molecules at these transition sites are released toward the plane of permeation. These rates will be obtained by multiplying the number of transition-site-attached molecules by the rate coefficient $k^{\ddagger}$ of the transition-state theory. Thus, the rate of release from the "upstream" side toward the central plane, q_-, will be positive (since it is in the direction of increasing x) and given by

$$q_- = k^{\ddagger}n_- \tag{25}$$

while from that from the "downstream" side toward the central plane, q_+, will be negative (since it is in the direction of decreasing x) and given by

$$q_+ = -k^{\ddagger}n_+ \tag{26}$$

so that the net rate of molecules flowing across the plane of permeation, q, will be the sum of these two rates:

$$q = q_+ + q_- = k^{\ddagger}(n_- - n_+) \tag{27}$$

Combining eqs. (24)–(27) gives the net molecular rate of permeation as

$$q = -Ak^{\ddagger}K^{\ddagger}\Delta p/b\lambda \tag{28}$$

Note that the central-plane depth d has disappeared, confirming that the rate is independent of this depth.

Dividing eq. (28) throughout by the Avogadro constant, N_A, gives the macroscopically observed rate, Q, that is, the amount (moles) of permeant passing across the layer in unit time, as

$$Q = -Ak^{\ddagger}K^{\ddagger}\Delta p/bN_A\lambda \tag{29}$$

Comparing this expression for Q obtained from the TSM with the standard expression for ideal permeation, eq. (1), shows that this TSM expression correctly incorporates the observed proportionalities of Q with the area, A, the pressure difference, Δp, and the reciprocal of the thickness, b. The permeability coefficient is thus given by

$$P = k^{\ddagger}K^{\ddagger}/N_A\lambda \tag{30}$$

Permeability Coefficient and Thermodynamics of the Insertion Process

The rate coefficient $k^{\ddagger}$ in the above expressions is given from transition-state theory as

$$k^{\ddagger} = k_B T/h \tag{31}$$

where k_B is the Boltzmann constant and h is the Planck constant.[50,51] The equilibrium constant $K^{\ddagger}$ can be expressed in thermodynamic terms by

$$K^{\ddagger} = \exp(-\Delta G^{\ddagger}/RT) \tag{32}$$

where $\Delta G^{\ddagger}$ is the standard free-energy change for the insertion process , that is, transferring 1 mol of permeant from the gas phase at unit pressure to 1 mol of the transition sites. Expanding the free energy into its enthalpy ($\Delta H^{\ddagger}$) and entropy ($\Delta S^{\ddagger}$) components and combining eqs. (30)–(32) gives

$$P = (k_B T/h\lambda N_A)\exp(-\Delta H^{\ddagger}/RT)\exp(\Delta S^{\ddagger}/R) \tag{33}$$

The enthalpy component may be further expanded as

$$\Delta H^{\ddagger} = \Delta U^{\ddagger} + p\Delta V^{\ddagger} \tag{34}$$

where $\Delta U^{\ddagger}$ and $\Delta V^{\ddagger}$ are the internal energy and volume changes for the transfer process, respectively. Since the volume change is that for the condensation of the 1 mol of gas onto the sites, then neglecting deviations from ideal gas behavior, and any volume effects at the transition site, this becomes

$$\Delta H^{\ddagger} = \Delta U^{\ddagger} + RT \tag{35}$$

Substituting in eq. (33) and rearranging slightly, this gives the TSM relation for the permeability coefficient:

$$P = (k_B T/ehN_A\lambda)\exp(\Delta S^{\ddagger}/R)\exp(-\Delta U^{\ddagger}/RT) \tag{36}$$

where e is the exponential number (derived from the factor RT in eq. (35)).

This TSM expression is seen to conform with the experimentally observed Arrhenius temperature dependence of the permeability coefficient, eq. (9). Equating the preexponential parts and the exponential parts of these two equations gives

$$P_A = (k_B T/ehN_A\lambda)\exp(\Delta S^{\ddagger}/R) \tag{37}$$

and

$$E_P = \Delta U^{\ddagger} \tag{38}$$

Considering eq. (37), evidently, the preexponential factor P_A is not expected to be truly temperature-independent, since it does contain T, but over the temperature ranges used, the variation is much less than that in the exponential factor, so that it is permissible to use the average absolute temperature in applying this equation. The entropy of activation $\Delta S^{\ddagger}$ can be expressed in terms of the entropies of the "reactants" and "products" as

$$\Delta S^{\ddagger} = S(\mathrm{GL}) - S(\mathrm{L}) - S^0(\mathrm{G}) \tag{39}$$

where S(GL) is the entropy of 1 mol of occupied sites; S(L), that of the vacant sites; and $S°$(G), the molar absolute entropy of the permeant gas G (see Appendix C). Substituting in eq. (37) and

transferring the absolute entropy term over to the left-hand side gives

$$P_A \exp[S^0(G)/R] = (k_B T/ehN_A\lambda)\exp\{[S(GL) - S(L)]/R\} \quad (40)$$

The quantity on the left-hand side is experimentally accessible, as are all the quantities on the left-hand side except for the intersite spacing (lattice parameter) λ and the entropy difference inside the exponential term. It is convenient to symbolize the left-hand side of eq. (40) by Y, that is:

$$Y \equiv P_A \exp[S^0(G)/R] \quad (41)$$

where this quantity Y may be termed the "entropy-adjusted Arrhenius preexponential factor" or, more simply, the "entropy function." For later application, substituting for Y in eq. (40) and taking logarithms gives

$$\log Y = \log(k_B T/ehN_A) - \log \lambda + (\log e)\{[S(GL) - S(L)]/R\} \quad (42)$$

Considering eq. (38), the activation energy for permeation is revealed as the internal energy change, $\Delta U^{\ddagger}$, required to expand the matrix of the polymer at the transition site L to accommodate the molecule of the permeant. Likewise, the difference $[S(GL)-S(L)]$ in eqs. (40)–(42) is the accompanying entropy change; for a polymer, it would be that associated with the altered conformations of the polymer chains around the transition site L when the molecule of the permeant is introduced.

Status of Permeation Versus Diffusion

Standing back for a moment from this mathematical jungle, the TSM has therefore led to a "decoupling" of the sorption process from the permeation process. Indeed, with this picture, it is now diffusion which is to be considered the secondary or derived quantity, with eq. (7) being inverted into the form

$$D = P/B \quad (43)$$

This is, of course, not to deny that the molecules of the permeant have to be absorbed by the polymer matrix, and to move by diffusive jumps, to arrive at some point inside the polymer, such as a transition site L. But it does indicate that from the molecular viewpoint, as well as in interpreting and predicting such behavior, the permeability coefficient has a simpler basis. In particular, the AJM for diffusion involves the features of the permeant molecule G at the sorption site and those for G at the transition site L—both of which are situations that are not clearly defined. By contrast, the TSM involves the equilibrium between the molecule in the gas or vapor (a generally well-defined and well-understood state) and that in the transition site L. Experimental data on permeation therefore enable us to use the permeant molecule to probe the properties of the transition sites, as shown later in the article.

Molecular Basis of Ideal and Nonideal Permeation

It is also possible to see why certain systems should show ideal permeation and others nonideal. If the amount of the permeant sorbed is small, then this will not affect the properties of the transition sites L, so that the permeation will be ideal. For high degrees of sorption, the sorbed permeant molecules are, on average, closer to transition sites L, so that a "plasticization" effect will change the thermodynamic character of the transition-site behavior. The "ideal permeation" behavior of water with moderately polar polymers already discussed may be ascribed to the water molecules being so strongly bound (hydrogen-bonded) to the sorption sites that they do not affect the transition sites L; the deviation from ideal sorption (Henry's Law) has conventionally been ascribed to "clustering," but, once again, this would tend to localize their radius of action that, therefore, does not extend to influencing the transition site L.

EFFECTS OF THE VARYING THE NATURE OF THE POLYMER AND THE PERMEANT

In the above development of the TSM, it has been assumed that we are dealing with a single polymer and a single permeant. In extending this to a range of polymers, and a range of permeants, there are three features that would be expected to vary: the nature of the transition site L; the value of the site-spacing λ; and the nature of the interactions between the polymer matrix at the transition site L and the permeant molecule. For example, even with a single polymer and a range of permeants, if there is a fixed type of transition

site L with a defined "hole size," then the smallest permeants (such as He) may pass through the hole so easily that it may not represent a barrier to it, while the larger quasi-spherical permeants, such as sulfur hexafluoride (SF_6), may be so large that they would not be able to pass through the barrier at all. Even for the more realistic picture of a range of hole sizes (and barrier heights), the smallest permeants would be using one end of the distribution and the larger ones the other end, so that the set of transition sites used by one group would be different from that used by the other group.

Furthermore, such considerations apply only for a particular choice of temperature, for example, one that is convenient experimentally, or that is important in the application of the polymer. This applies to the single-temperature correlation of Stannett and Szwarc and the "Permachor" concept of Salame that were considered earlier.

From the more fundamental viewpoint, therefore, we have to consider the temperature-independent quantities, that is, the Arrhenius parameters. It should be possible to use these to probe the mechanical and thermodynamic characteristics of the polymer transition site L, which must not be expected to be the same as that of the bulk of the polymer. To this end, it is necessary to choose a suitable dataset of polymers and permeants from the literature.

DATASET OF ARRHENIUS PARAMETERS FOR PERMEATION

Source of the Arrhenius Parameter Data

The TSM theory has been tested by applying it to the literature permeation data compiled by Pauly in the *Polymer Handbook*.[6] These data are evidently accepted as authoritative and may, in most cases, be confirmed by referring back to the original articles.

Polymers in the Dataset

Focusing on homopolymers, 16 such polymers were found in the *Polymer Handbook* compilation[6] for which the Arrhenius parameters for permeation were determined for at least four "simple" permeants (see below), so as to make them suitable for further analysis—in particular, to look for linear correlations in the four test plots used.

The characteristics of these 16 polymers are listed in Table II, where they are given the code letters **A** through **P**. They comprise five hydrocarbon polymers—natural rubber (**A**), polydimethylbutadiene (**D**), three PEs (**F**, **G,** and **H**), and polypropylene (**L**); three vinyl polymers—PVAC (**N**), PVBZ (**O**), and PVC (**P**); a methacrylate ester, PEMA (**J**); two fluorinated polymers, PETFE (**I**) and PTFE (**M**); two chain heteraoatomic polymers PA (nylon 11) (**B**) and PET (**K**); and a silicone polymer, PDMS (**E**). With one exception, they are all true homopolymers; even the apparent exception, PETFE (**I**), is seemingly an alternating copolymer and, hence, can be viewed as a homopolymer of the combined repeat unit.[60]

Although the present theory is aimed at amorphous polymers, many of the polymers in the dataset are semicrystalline; also, the sample PDMS (**E**) is reported to have a minor content (10%) of filler (Table II). This will affect their permeability coefficients. However, because of uncertainties in the actual amorphous contents, and because of uncertainties in the effects of crystallinity and fillers on permeation, no attempt has been made to "correct" the permeation parameters to those for fully amorphous polymers.[1,69]

Permeants in the Dataset

The "simple" permeants for which Arrhenius parameter data are available comprise also (almost coincidentally) 16 gases that are listed in Table III in the order of the molecular weight, M_G, with code letters **a**–**p** and with other properties and characteristics that are important here. These comprise the five noble gases He (**b**), Ne (**d**), Ar (**i**), Kr (**m**), and Xe (**o**); the six diatomic gases H_2 (**a**), N_2 (**e**), CO (**f**), O_2 (**g**), HCl (**h**), and Cl_2 (**l**); the two triatomic gases CO_2 (**j**) and SO_2 (**k**); and the three polyatomic molecules CH_4 (**c**), SiF_4 (**n**), and SF_6 (**p**). These permeants should have effectively spherical molecules. This is evidently the case with the noble gases, and it is ensured by free rotation at these temperatures with the diatomic molecules, and with the last three polyatomic molecules because of their high symmetry, although it becomes somewhat less sure with the "elongated" cases of the triatomic gases CO_2 (**j**) (which has a linear molecule) and SO_2 (**k**) (which has an angular molecule).[70]

In addition, data for water vapor [H_2O (**w**)] are included where they are available for the same polymer sample; this permeant is considered separately from the other permeants because its permeation behavior is also clearly different.

Table II Features of the 16 Polymer Samples

				T_g		Glass: $T < T_g$			Rubber: $T > T_g$		
#	M	Monomer Unit	ϕ_a	Ref	Lit	T_{min}	T_{max}	T_{ave}	T_{min}	T_{max}	T_{ave}
A	NR[a]	—CH_2—CH═CMe—CH_2—	1.00	?	203	?	?	?	293	323	308
B	PA[b]	—NH—CO—$(CH_2)_{10}$—	0.80	?	315	283	315	299	315	333	324
C	PC[c]	—O—CO—O—Ph—CMe_2—Ph—	1.00	398	418	273	398	336	398	448	423
D	PDMB[d]	—CH_2—CMe═CMe—CH_2—	1.00	?	262	?	?	?	298	323	310
E	PDMS[e]	—$SiMe_2$—O—	1.00	?	146	?	?	?	233	298	266
F	PE1[f]	—CH_2—CH_2—	0.23	?	148	?	?	?	278	333	306
G	PE2[g]	—CH_2—CH_2—	0.57	?	148	?	?	?	278	333	306
H	PE3[h]	—CH_2—CH_2—	0.71	?	148	?	?	?	278	333	306
I	PETFE[i]	—CH_2—CH_2—CF_2—CF_2—	0.50	328	?	278	328	303	328	373	350
J	PEMA[j]	—CH_2—CMe(CO—O—Et)—	1.00	338	338	298	338	318	338	353	346
K	PET[k]	—O—$(CH_2)_2$—O—CO—Ph—CO—	0.60	353	342	293	353	323	353	403	378
L	PP[l]	—CH_2—CHMe—	0.52	?	260	?	?	?	303	328	316
M	PTFE[m]	—CF_2—CF_2—	0.50	?	?	278	373	326	278	373	326
N	PVAC[n]	—CH_2—CH(O—CO—Me)—	1.00	296	305	273	296	284	296	313	304
O	PVBZ[o]	—CH_2—CH(O—CO—Ph)—	1.00	333	344	293	333	313	333	358	346
P	PVC[p]	—CH_2—CHCl—	1.00	348	354	298	348	323	348	363	356

#, polymer code; M, polymer acronym—details in footnotes a–p below; ϕ_a, volume fraction amorphous content of the sample; T_g, Ref: glass transition temperature from the original reference (footnotes a–p), Lit: glass transition temperature from the literature.[54] T_{min}, T_{max}, and T_{ave}, minimum, maximum, and average experimental temperature for all the permeants studied with the sample. ?, no data available.

[a] NR: natural rubber, *cis*-polyisoprene; unvulcanized smoked sheet Hevea; data of Michaels and Bixler.[55,56]

[b] PA: polyamide (Nylon) 11, poly(imino-1-oxoundecamethylene); data of Ash et al.[57]

[c] PC: polycarbonate, poly(oxycarbonyloxy-1,4-phenyleneisopropylidene-1,4-phenylene); General Electric "Lexan"; data of Norton.[58]

[d] PDMB: poly(2,3-dimethylbutadiene), "methyl rubber"; data compiled by Pauly.[6]

[e] PDMS: polydimethylsiloxane, vulcanized, with 10% Santocel CS filler; data of Barrer and Chio[59]; Arrhenius parameters recalculated, correcting an error in the P_A value for Ar.

[f] PE1: high-density polyethylene (HDPE); Grace "Grex", ρ = 0.9640 g cm^{-3}, 0.15% Me groups; data of Michaels and Bixler.[55,56]

[g] PE2: low-density polyethylene (LDPE); DuPont "Alathon 14", ρ = 0.9137 g cm^{-3}, 3% Me groups; data of Michaels and Bixler.[55,56]

[h] PE3: hydrogenated polybutadiene (HPBD); Phillips "Hydropol", ρ = 0.8940 g cm^{-3}, 5% Me groups, 1.3% C═C; data of Michaels and Bixler.[55,56]

[i] PETFE: poly(ethylene-*alt*-tetrafluoroethylene); Hoechst "Hostaflon ET"; ϕ_a = 0.50 value assumed; T_g value taken from the fact that different parameters for H_2O are quoted below and above this temperature (no literature value found); data of Pauly[6]; the alternating structure was presumed from another literature source.[60]

[j] PEMA: poly(ethyl methacrylate); data of Stannett and Williams[29]; parameters for SiF_4 estimated from their graph.

[k] PET: poly(ethylene terephthalate); data of Michaels et al.[61,62]

[l] PP: polypropylene; pooled closely similar data for three polymers with ρ = 0.893 ± 0.006 g cm^{-3}, ϕ_a = 0.50 ± 008; data of Sezi and Springer.[63]

[m] PTFE: polytetrafluoroethylene; Hoechst "Hostaflon FPA"; data of Pauly[6]; there are two values of T_g (260 and 400 K) quoted in the literature,[54,64] so that the polymer is taken to be in either state for the present purposes.

[n] PVAC: poly(vinyl acetate); data of Meares.[65,66]

[o] PVBZ: poly(vinyl benzoate); data of Hirose et al.[67]; value of P_A for Xe above T_g corrected—the quoted value[67] is 100-fold too high.

[p] PVC: poly(vinyl chloride); unplasticized sample; data of Tikhomirov et al.[68]; the data are mainly below T_g, and the values above T_g are therefore less certain; the Arrhenius parameters for Ar were recalculated for the temperature ranges above and below T_g.

Glass Transition Behavior in the Dataset

As noted earlier, the behavior of the permeation with regard to the glass transition temperature (T_g) is often complex. In particular, the Arrhenius plot may show a break at the T_g, giving different values of the Arrhenius parameters for the glass state (below T_g) and the rubber state (above T_g).

In the present case, seven of the polymers in the dataset—NR (**A**), PDMB (**D**), PDMS (**E**), PE1 (**F**), PE2 (**G**), PE3 (**H**), and PP (**L**)—had been studied only above the T_g, so that no comparisons between these two states can be drawn.

Furthermore, with PTFE (**M**), there is considerable uncertainty of interpretation because

Table III Characteristics of the Permeant Gases and Vapors, G, in Order of Their Relative Molar Mass

#	G	M_G	ΣZ	b	σ_G	S^0	Class
a	H_2	2.0	2	26.51	276	226	Small
b	He	4.0	2	23.80	266	222	Small
c	CH_4	16.0	10	43.01	324	282	Small
d	Ne	20.2	10	26.51[a]	276[a]	242	Small
e	N_2	28.0	14	38.70	313	287	Small
f	CO	28.0	14	39.48	315	294	Small
g	O_2	32.0	16	31.86	293	256[b]	Small
h	HCl	36.5	18	40.61	318	283	Small
i	Ar	40.0	18	32.01	294	251	Small
j	CO_2	44.0	22	42.86	324	310	Large
k	SO_2	64.1	32	56.79	356	344	Large
l	Cl_2	70.9	34	54.22	350	319	Large
m	Kr	83.8	36	39.60	315	260	Small
n	SiF_4	104.1	50	72.36	386	379	Large
o	Xe	131.3	54	51.56	344	266	Large
p	SF_6	146.1	70	87.86	411	387	Large
w	H_2O	18.0	10	30.49	289	285	Small

#, code letter; G, molecular formula; M_G, relative molar mass; ΣZ, summed atomic numbers of component atoms (total number of electrons); b, van der Waals covolume ($cm^3\ mol^{-1}$)—see Appendix B; σ_G, van der Waals molecular diameter (pm)—see Appendix B; S^0, absolute entropy ($J\ K^{-1}\ mol^{-1}$ ⟨Pa⟩)—see Appendix C; Class, size classification ("small" or "large") for the permeation plots—see text.

[a] See Appendix B for the assignment of these values.

[b] See Appendix C for the assignment of this value.

there are two reported glass transition temperatures (260 and 400 K), along with multiplicity of "crystalline transitions" for the polymer.[54,64] To avoid having to make a decision in this case, it has been treated as having the same parameters below and above the T_g, as with case (a) below, but with the conclusions to be interpreted bearing in mind this assumption.

For the remaining eight polymers, three cases can be distinguished: (a) PA (**B**), and PVC (**P**): There was no break with any of the gases studied, except that in the case of PVC the data for Ar (**i**) and Kr (**m**) did show a break; (b) PETFE (**I**) and PEMA (**J**): There was no break with any of the gases, but a break with H_2O (**w**) which may be taken to define the value of T_g; (c) PC (**C**), PET (**K**), PVAC (**N**), and PVBZ (**O**): There was a break at T_g for all the gases studied.

THE FOUR TYPES OF TEST PLOTS USED

Four types of plots—designated Type 1, Type 2, Type 3, and Type 4 plots—were used in examining the literature data of the polymer/permeant data set and for fitting linear regression relations where they seemed justified by the graphs obtained. These plots involved the Arrhenius parameters P_A (plotted as $\log P_A$) and E_P, along with the entropy function Y (plotted as $\log Y$) and the permeant molecular diameter σ_G (Table III and Appendix B).

Type 1 Plot: Log P_A Against Activation Energy E_P

Background

In studies of the diffusion in polymers, when a particular polymer is used with a range of permeants, a linear correlation is often found between the Arrhenius quantities for diffusion, $\log D_A$ and E_D, obtained from eq. (10).[1,14,16,59,66] This type of correlation is commonplace in kinetics and thermodynamics, going by such names as the "compensation rule" and the "isokinetic relationship," as discussed below. This Type 1 plot is, therefore, a test for the behavior of the Arrhenius parameters for permeation and does not at this stage involve the TSM directly, except to act as comparison with the later plots.

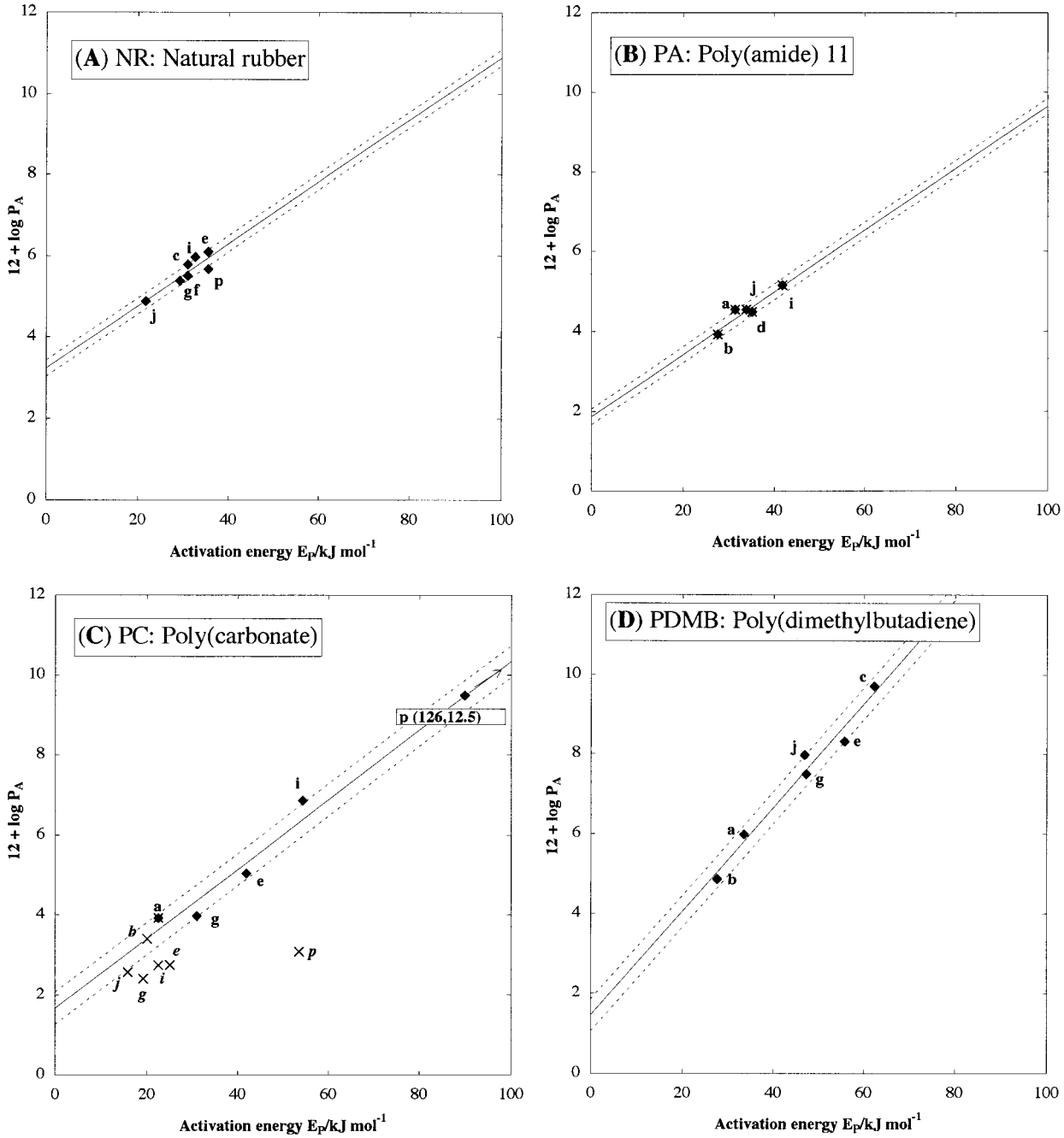

Figure 4 (A–P) Type 1 plots (Arrhenius parameters): log P_A versus activation energy E_P; polymers as Table II, permeants as Table III. (×) glass state ($T < T_g$); (♦) rubber state ($T > T_g$).

Results

The plots are shown for the present dataset in Figure 4(A–P), with common scales for ease of comparison. Where such a plot is linear, it may be fitted by the standard regression equation

$$\log P_A = m_1 E_P + c_1 \qquad (44)$$

The derived values of the regression parameters are listed in Table IV.

Isokinetic Temperatures

The term isokinetic relationship implies that for a specific polymer there is a particular temperature, the "isokinetic temperature," T_i, at which

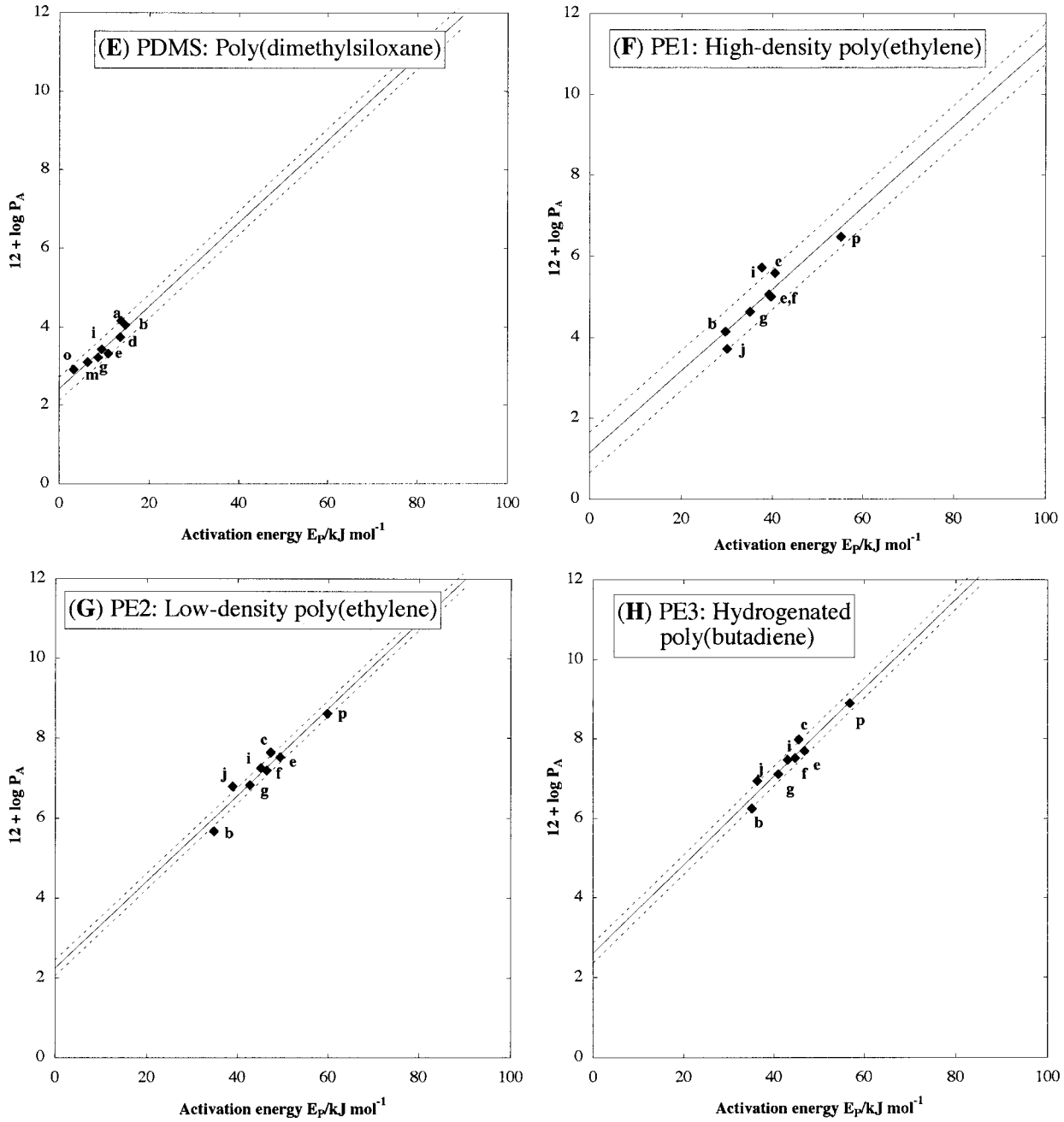

Figure 4 Type 1 plots (Arrhenius parameters) (*Continued from the previous page*)

opposing effects of the two factors, $\log P_A$ and E_P, cancel out and the permeability coefficient has the same value, P_i, for all the permeants. It may be evaluated by comparing eq. (44) with the logarithmic form of the Arrhenius relation, eq. (9), at this temperature:

$$\log P_i = \log P_A - E_P(\log e)/RT_i \qquad (45)$$

which also represents a linear relation between $\log P_A$ and E_P. This, therefore, gives

$$T_i = (\log e)/m_1 R \qquad (46)$$

The value of T_i may or may not be within the experimentally accessible range. However, if T_i is similar to the average temperature, T_{ave},

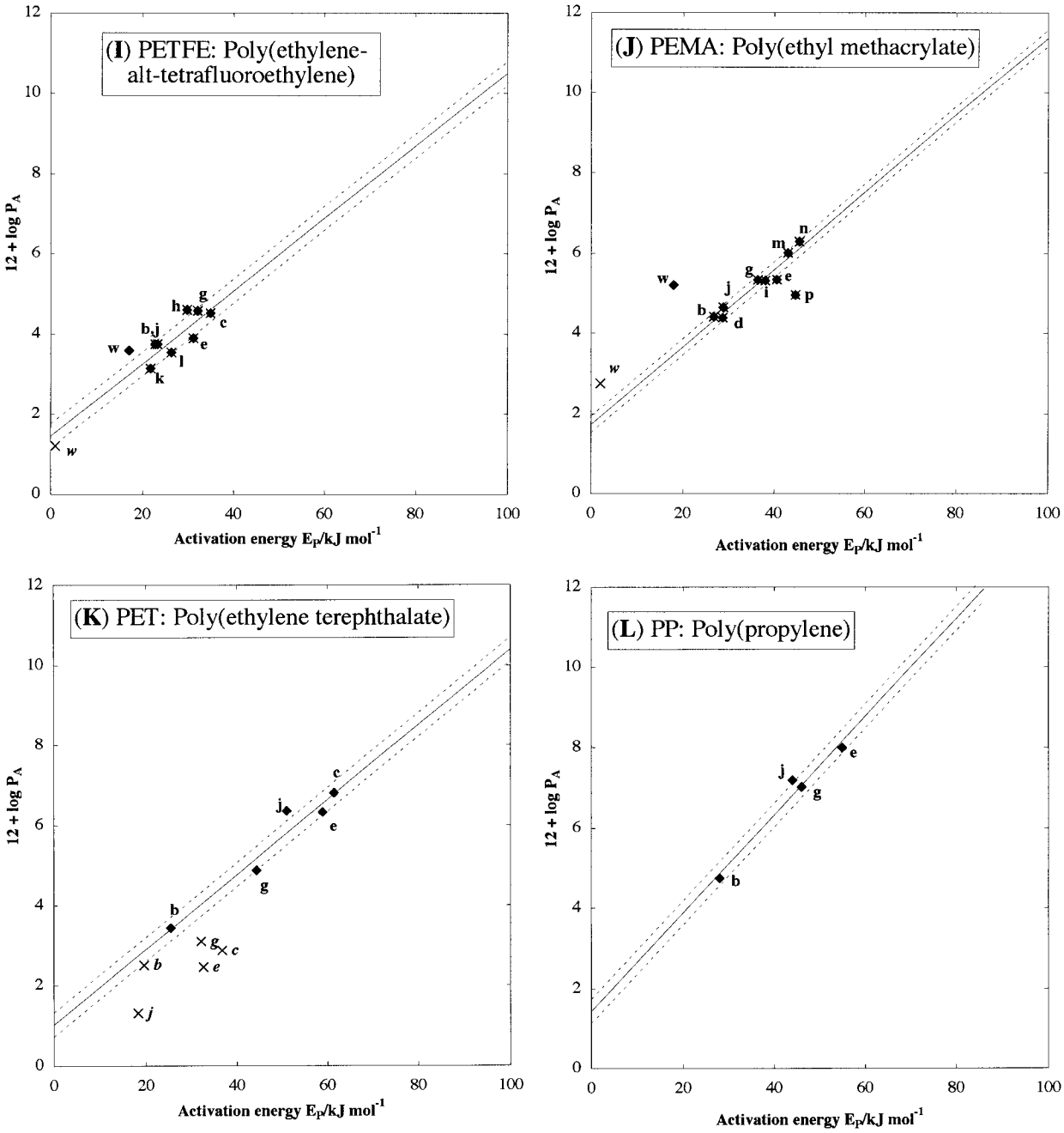

Figure 4 Type 1 plots (Arrhenius parameters) (*Continued from the previous page*)

then this suggests that the correlation is spurious, arising from "random fluctuations" in the estimated parameters—if the intercept of the plot is overestimated, then the slope will be underestimated in a correlated fashion and vice versa.

Correlation Behavior

Considering first the behavior for polymers in the rubber state ($T > T_g$) (filled diamond symbols) from the broken-line bands (corresponding to ± 0.25 units on the ordinate scale), the plots in Figure 4 are seen to be reasonably linear. The correlation coefficient r_1 (Table IV) averages 0.95, the highest values being 0.992-0.996 for PC (**C**), PVAC (**N**) and PVC (**P**); the poorest correlations are seen with NR (**A**), 889 and PETFE (**I**), 0.823. The low r values may be related to the restricted span of the plotted values, coupled with the fixed spread about the

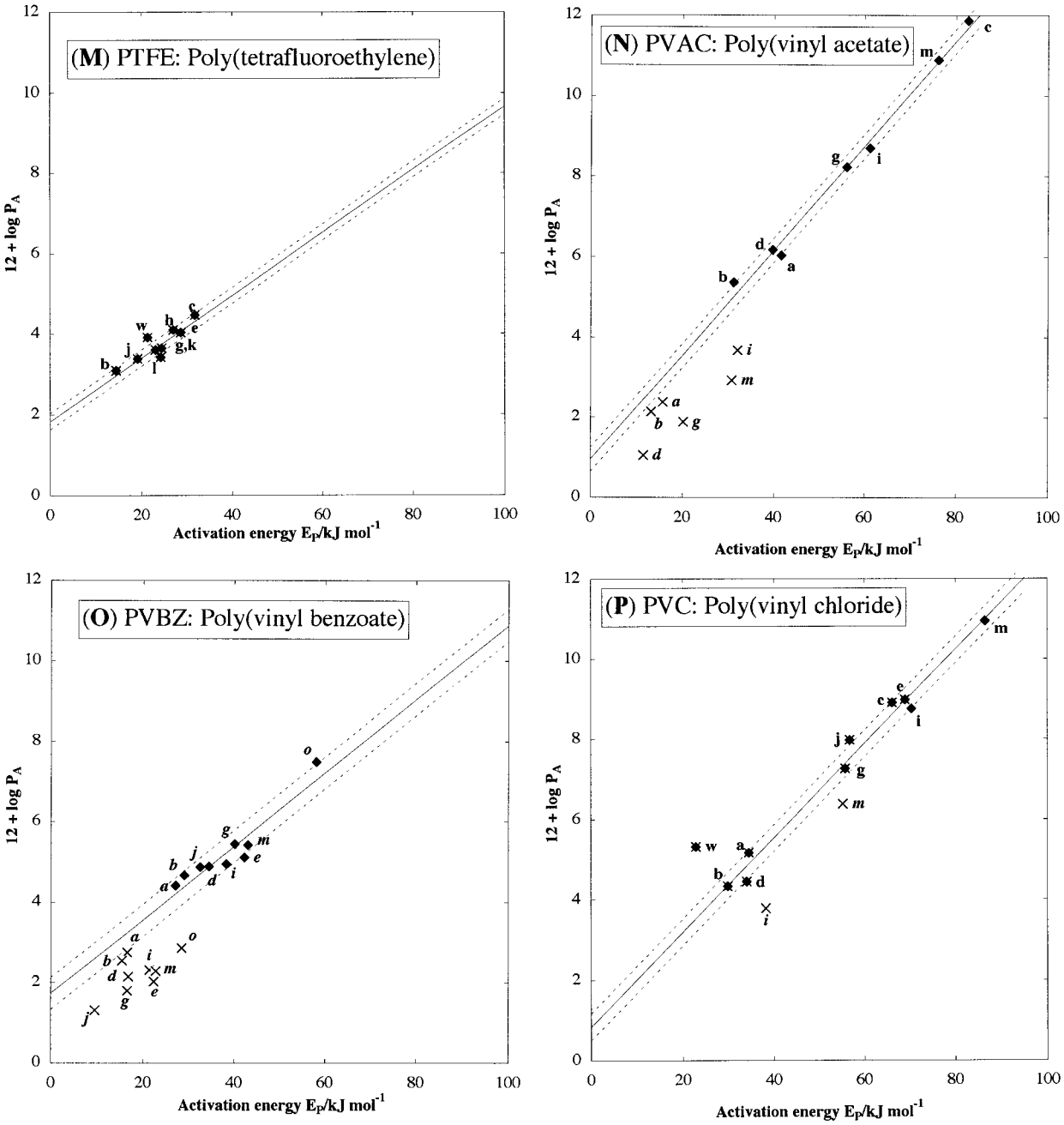

Figure 4 Type 1 plots (Arrhenius parameters) (*Continued from the previous page*)

regression line. Since these systems are believed to have reliable permeation data, and we wish to have an objective view of the behavior and of the acceptability of the present theory to polymers in general, we will not reject these from further consideration, but accept the isokinetic parameters derived along with their correspondingly greater uncertainties.

For the polymers in the glass state ($T < T_g$), where there is no break at the T_g, then the correlation coefficients are as for the rubber state Table IV), with a low of 0.823 for PETFE (**I**). In the cases where there is a break, the correlations are much poorer, with values ranging from 0.863 for PVAC (**N**) down to 0.152 for PC (**C**). These low values must be taken to indicate the absence of any overall correlations for the permeants in general.

If we accept that there is no such overall correlation in the glass state, then the values of the

Table IV Type 1 Plot: Parameters for the Linear Correlations Between log P_A and the Permeation Activation Energy E_P

		Glass State: $T < T_g$			Rubber State: $T > T_g$				
#	Polymer	r_1	c_1	m_1	r_1	c_1	m_1	T_i	T_i/T_{ave}
A	NR	?	?	?	0.889	3.23(55)	0.077(18)	678	2.20
B	PA	0.948	1.88(52)	0.078(15)	0.948	1.88(52)	0.078(15)	670	2.17
C	PC	0.152	*	*	0.996	1.67(25)	0.087(4)	600	1.42
D	PDMB	?	?	?	0.986	1.46(52)	0.130(11)	402	1.30
E	PDMS	?	?	?	0.904	2.43(19)	0.105(17)	562	2.11
F	PE1	?	?	?	0.904	1.16(76)	0.101(20)	522	1.71
G	PE2	?	?	?	0.964	3.10(48)	0.108(12)	574	1.88
H	PE3	?	?	?	0.967	2.61(53)	0.111(12)	528	1.73
I	PETFE	0.823	1.46(71)	0.090(25)	0.823	1.46(71)	0.090(25)	528	1.51
J	PEMA	0.973	1.74(34)	0.096(9)	0.973	1.74(34)	0.096(9)	544	1.57
K	PET	0.737	*	*	0.971	1.02(66)	0.094(13)	556	1.47
L	PP	?	?	?	0.985	1.44(68)	0.122(15)	428	1.35
M	PTFE	0.941	1.83(31)	0.078(13)	0.941	1.83(31)	0.078(13)	670	2.06
N	PVAC	0.863	*	*	0.996	0.95(31)	0.130(5)	402	1.32
O	PVBZ	0.628	*	*	0.943	3.04(37)	0.091(12)	574	1.66
P	PVC	0.992	0.84(34)	0.117(6)	0.992	0.84(34)	0.117(6)	446	1.25

See Table II for the polymer codes and details of the samples used. See Figure 4(A–P) for the respective plots. r_1, correlation coefficient; c_1, ordinate intercept—eq. (44); m_1, gradient—eq. (44); T_i, isokinetic temperature (K)—eq. (46); T_{ave}, average experimental temperature (K) for the rubber state (Table III). ?, no data available—sample not studied in this state; *, no meaningful data—poor linear correlation.

correlation coefficient obtained are indicative of the spurious correlation due to the isokinetic temperature being close to the (mean) experimental temperature.

The values of the regression parameters are plotted as a "scattergram" in Figure 5. It is difficult to see any clear correlation between the plotted values or any correlation with the structure of the repeat units of the polymers. Nevertheless, these parameters may be taken to be characteristic quantities for the particular polymer for any permeant.

However, all this having been said, we have to take note of the fact that the later Type 3 plots, where the preexponential factor P_A has been modified into the entropy function Y according to eq. (41), show better linear correlations, at least for the smaller-size permeants. This casts some doubts on any of the correlations apparently seen with these Type 1 plots, as discussed above.

Type 2 Plots: Activation Energy E_P versus Permeant Molecular Diameter σ_G

Background

One popular approach in interpreting diffusion data is to seek to correlate the activation energies for diffusion with the molecular diameters of the permeant molecules, or some power of this; the molecular basis of this has, however, always been rather tenuous.[1,44,56,58,62,65–68] In the present case with the transition-site model for permeation, evidently, the molecule must be expected to stretch the transition site L to accommodate itself; this would be expected to require a greater amount of energy, the greater the diameter of the molecule.

Results

The Type 2 plots of E_P versus the permeant molecular diameter σ_G for the 16 polymers are shown in Figures 6(A–P), with common scales for ease of comparison. For all the polymers except NR (**A**), PDMS (**E**), and PETFE (**I**), the Type 2 plots are linear with a positive slope, at least for the "small" molecules, that is, up to and including CH_4 (**c**) with σ_G = 324 pm, but excluding CO_2 (**j**) with nominally the same value of σ_G (Table III). This applies both above and below the glass transition temperature. There is a clear distinction here between the 10 "small" permeants (lying close to the regression lines) and the six "large" permeants (lying well away from the lines). With NR (**A**) and PETFE (**I**), no clear regression lines

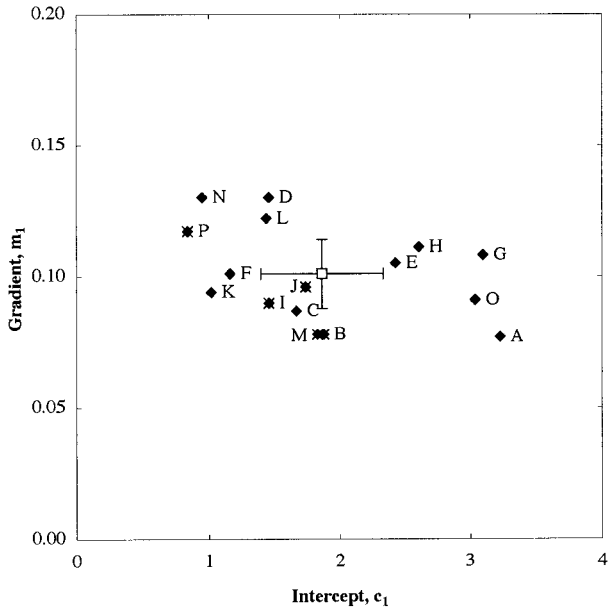

Figure 5 Linear regression parameters m_1 and c_1 for the Type 1 plots. Polymer codes as in Table II. (□) Mean point with mean standard deviation error bars; other symbols as Figure 4(A–P).

can be seen; with PDMS (**E**), the line has a negative slope.

The standard regression equation here is

$$E_P = m_2\sigma_G + c_2 \tag{47}$$

The derived values of the regression parameters are listed in Table V.

Even without entering into a molecular interpretation of this data, the close fit to the straight lines seen in Fig. 6 with the "small" molecules and 11 of the polymers—PA (**B**), PDMB (**D**), PE1 (**F**), PE2 (**G**), PE3 (**H**), PEMA (**J**), PET (**K**), PP (**L**), PTFE (**M**), PVAC (**N**), PVBZ (**O**)—gives us confidence both in the values of the molecular diameter for these molecules (Appendix B) and in literature values of the activation energy E_P for these systems.

Molecular Interpretation of the Type 2 Plots

The simplest interpretation of these linear plots (Figure 6) is that, for any particular polymer, the permeants on the line all use the same set of transition sites. The value of E_P represents the energy to expand the aperture to accommodate the molecule [eq.(38)]. The intercept on the molecular diameter axis, corresponding to the aperture size for zero activation energy, thus represents the size of the unperturbed aperture, σ_L; the average value of σ_L for the polymers [excepting PDMS (**E**) and the three PEs (**F**, **G**, **H**)] is 210(48) pm (Table VI). The permeant molecules evidently behave here as "hard spheres" of the stated van der Waals diameter σ_G. The slope of the line then represents the energy to expand the aperture to accommodate the increasingly large molecules, and its linearity shows that this involves a fixed "force constant" θ. To evaluate this from the gradient m_2 from eq. (47), which is in units of (kJ mol^{-1})/(pm/molecule), it is necessary to convert to a molecular basis throughout by introducing the Avogadro constant N_A (6.023×10^{23} molecules mol^{-1}) as well as to convert to consistent SI units (kJ → J, pm → m). This gives

$$\theta = 1.66m_2 \text{ nN} \tag{48}$$

where nN is nanonewtons. The derived values of θ are listed in Table VI. Excluding again PDMS (**E**) and the three PEs (**F**, **G**, **H**), the 10 polymers remaining give a mean value for θ of 1.00(43) nN; for the three PEs (**F**, **G**, **H**), this mean is 0.34(4) nN.

One curious feature of the parameter θ is that it represents a constant *force*, rather than a Hooke's Law/Young's modulus coefficient as might have been expected. It is as if the permeant molecule being inserted into the transition-site aperture were lifting a fixed weight.

Regarding the effect of the glass transition, there are five polymers that show different behavior below and above T_g: PC (**C**), PET (**K**), PVAC (**N**), PVBZ (**O**), and PVC (**P**). Here, although there are differences between the derived σ_L values (Table VI), these are within the limits of error of the intercepts on the molecular diameter axis (Fig. 6), indicating the same set of sites acts above and below T_g. This is shown more clearly by the results from the later plots.

Type 3 Plot: Log Y Against Activation Energy E_P

Background

These plots are similar to those in Type 1 plots for the Arrhenius parameters, but in this case, the values of the preexponential parameter P_A were "adjusted" by introducing the absolute entropy of the permeant, $S^0(G)$ to give the entropy function Y as defined by eq. (41).

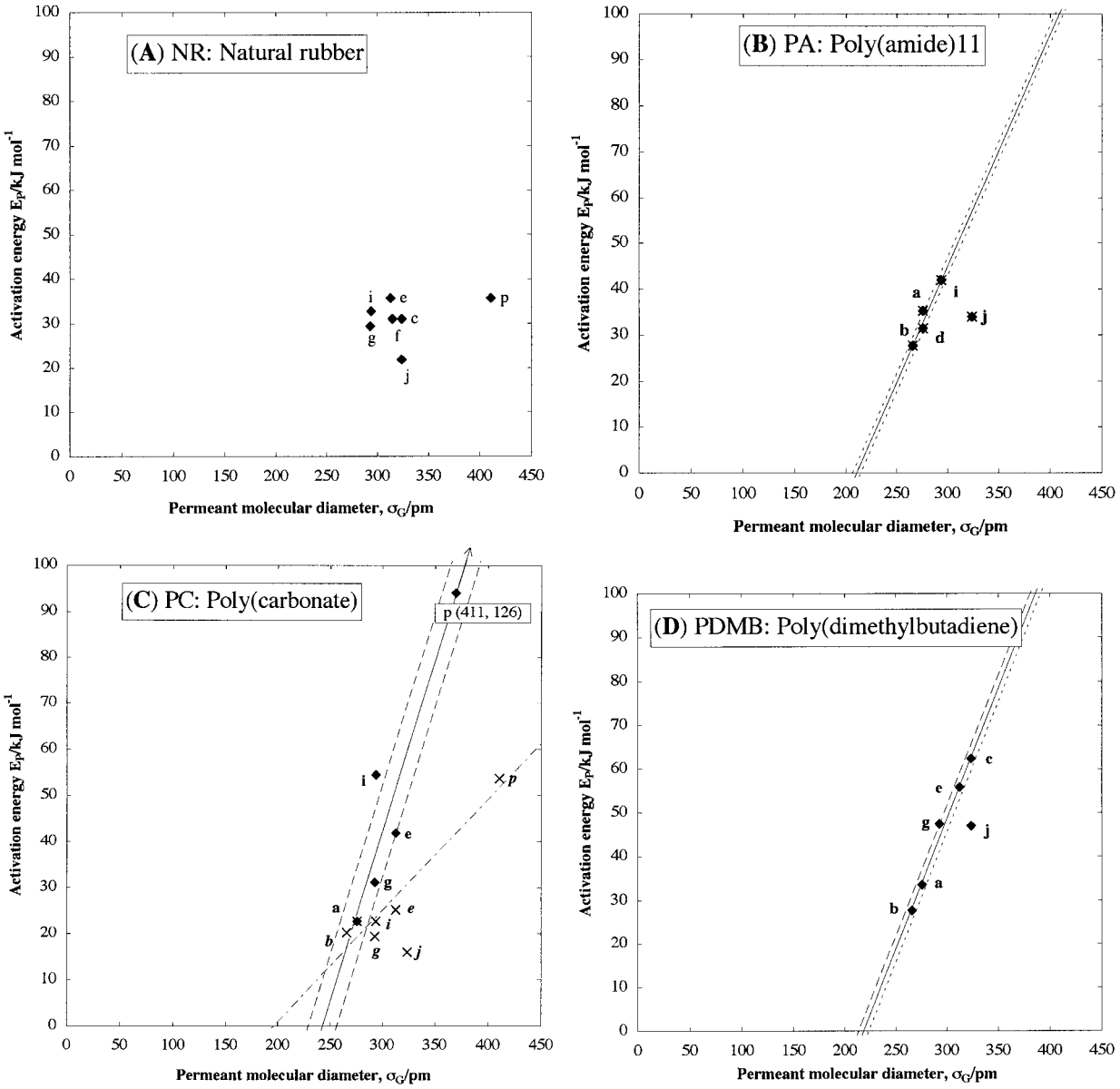

Figure 6 (A–P) Type 2 plots: permeation activation energy E_P versus permeant molecular diameter σ_G; polymers, permeants, and symbols as in Figures 4(A–P).

Results

The plots for the 16 polymers are shown in Figure 7(A–P), with common scales for ease of comparison. The pattern of behavior is similar to that seen with the Type 2 plots, with straight lines of positive slope except for NR (**A**), PDMS (**E**), and PETFE (**I**); with NR (**A**) and PETFE (**I**), there is again apparently only a cluster of points, while with PDMS (**E**), the line has again a negative slope. As before, there is a distinction between the 10 "small" permeants and the six "large" ones [CO_2 (**j**) and larger]. It is particularly remarkable that with four of the polymers, PET (**K**), PVAC (**N**), PVBZ (**O**), and PVC (**P**), where the parameters differ for the glass and rubber states, the points in these plots (Fig. 7) are brought onto an essentially common single line; this is not the case, however, with the corresponding fifth polymer, PC (**C**), although the data are evidently not as precise here as with the other polymers.

The standard form of the regression equation here is

$$\log Y = m_3 E_P + c_3 \qquad (49)$$

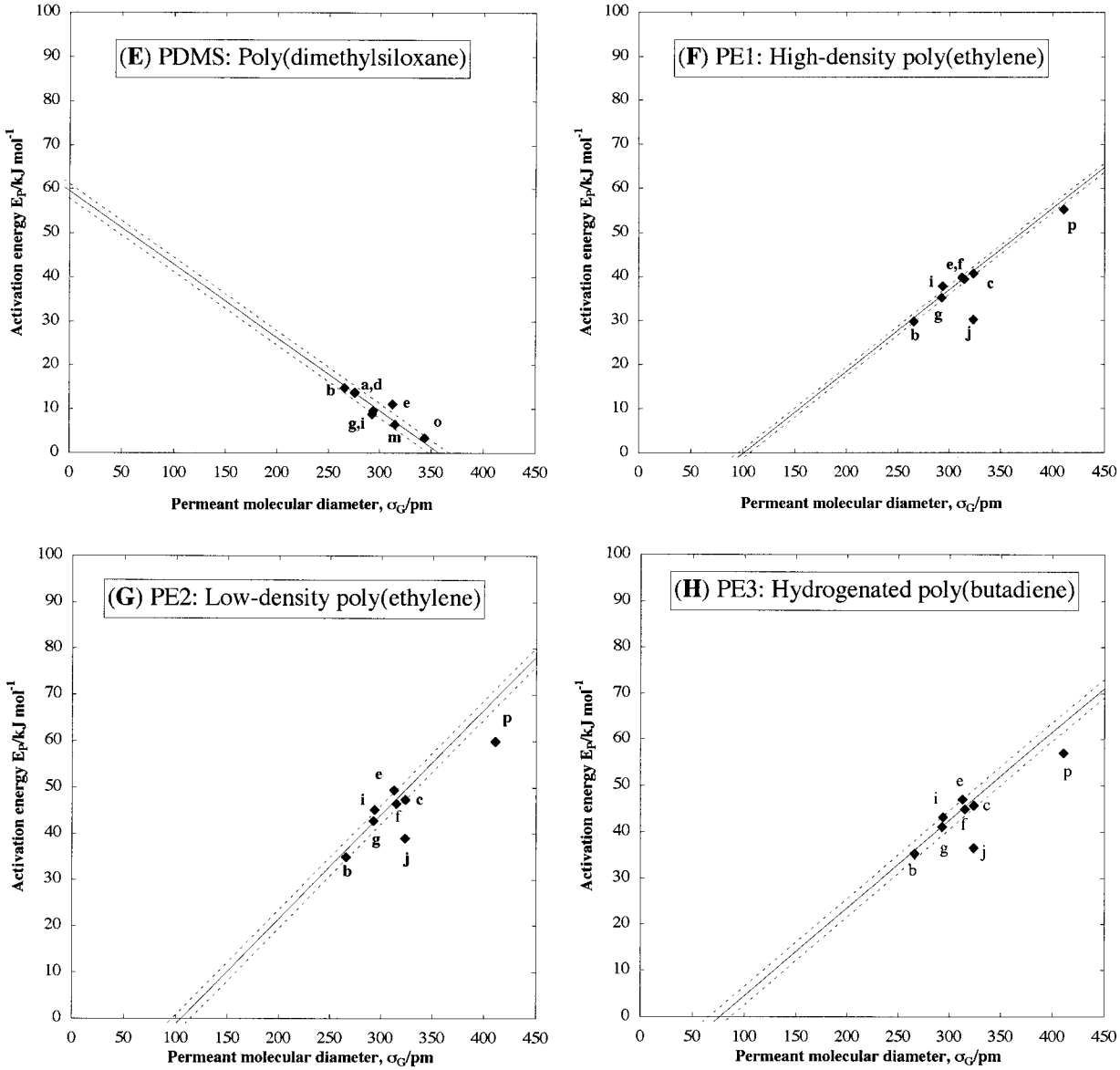

Figure 6 Type 2 plots (*Continued from the previous page*)

The linear regression parameters m_3 and c_3 are listed in Table VII.

As with the Type 2 plots, the close fit to straight lines seen in Figure 7 with the 10 "small" molecules and 12 of the polymers—PA (**B**), PDMB (**D**), PE1 (**F**), PE2 (**G**), PE3 (**H**), PEMA (**J**), PET (**K**), PP (**L**), PTFE (**M**), PVAC (**N**), PVBZ (**O**), and PVC(**P**)—gives us confidence in the Arrhenius parameters for these systems.

Even disregarding for a moment any theoretical basis for this Type 3 plot, it evidently gives a better correlation than does the Type 1 plot, the average value of the correlation coefficient (for the 11 polymers) being 0.98(2) This is not a completely fair basis of comparison because it involves omitting the "large" permeants from the correlations, although these are clearly distinguished from the "small" permeants.

Molecular Interpretation of the Type 3 Plots

The behavior seen from the plots in Figure 7(A–P) confirms the molecular interpretation for the Type 2 plots, that is, with a particular polymer, there is a single type of transition site for all the "small" permeants. The common lines obtained where the permeation parameters differ on either side of the glass transition temperature also con-

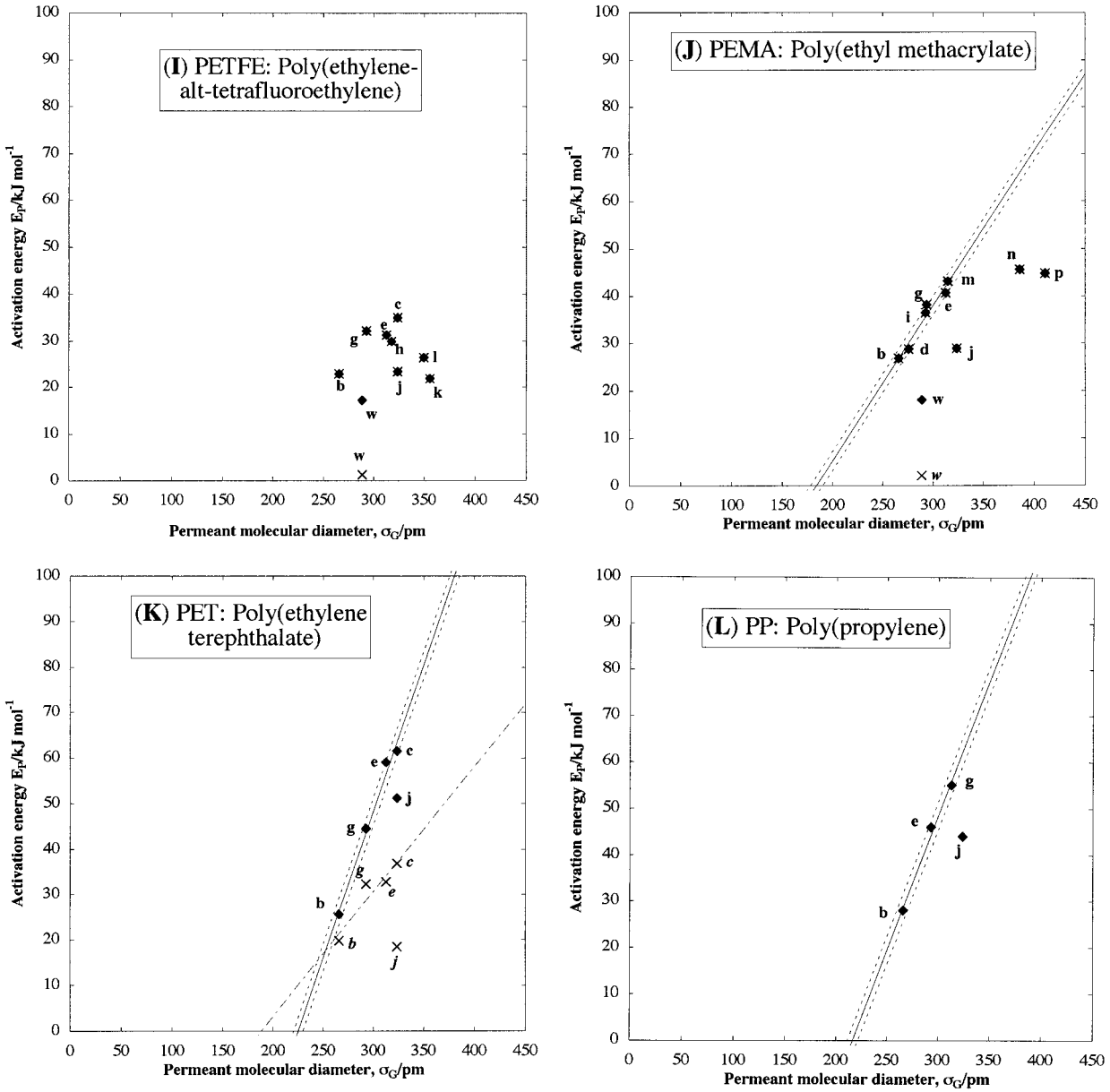

Figure 6 Type 2 plots (*Continued from the previous page*)

firm that the same set of transition sites is involved in the two states (glass and rubber) for these polymers.

This also enables us to obtain an estimate of the site-spacing λ, as follows: Comparing eqs. (42) and (49), the ordinate intercept c_3 is $\log Y_Z$, where Y_Z is the value of the entropy function Y for zero activation energy. Under these circumstances, the permeant molecule would have the same diameter as that of the transition-site aperture [this is, of course, a hypothetical situation, since He (**b**), the smallest molecule possible, is always larger than the transition-site apertures]. There is then no perturbation of the nearby polymer matrix, and the permeant molecule is held by the transition site with its translational entropic freedom removed, so that the factor $[S(\mathrm{GL}) - S(\mathrm{L})]$ becomes zero, and, hence, eq. (42) becomes

$$\log Y_Z = \log(k_B T/ehN_A) - \log \lambda \qquad (50)$$

Taking antilogarithms and rearranging this gives

$$\lambda = (k_B T/ehN_A)(Y_Z)^{-1} \qquad (51)$$

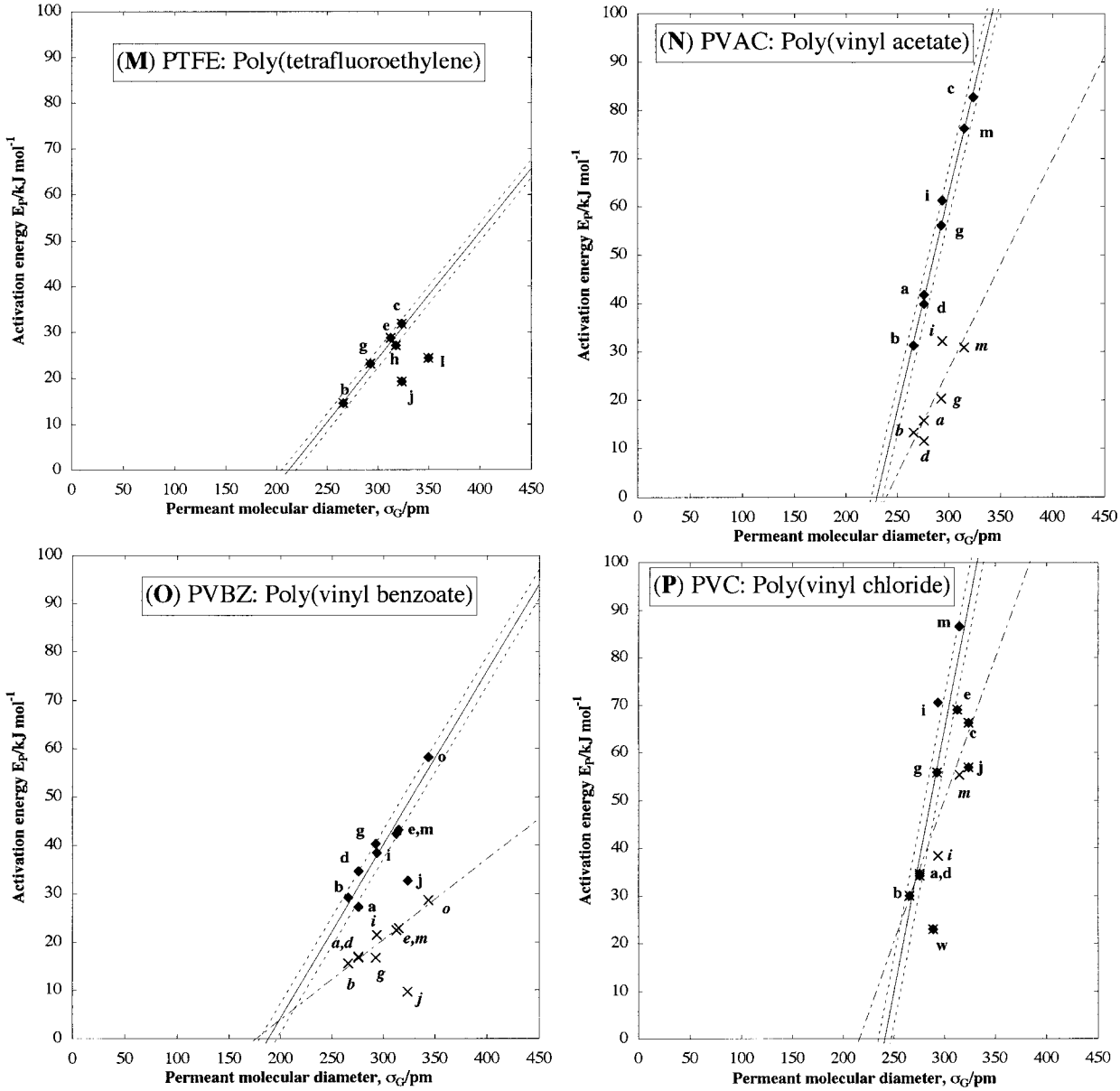

Figure 6 Type 2 plots (*Continued from the previous page*)

As with the interpretation of the Type 2 plots (above) and the Type 4 plots (below), it is necessary to convert this to a molecular basis by introducing the Avogadro constant, as well as converting the "standard" units of Y (Appendix A) into SI units by introducing the molar gas volume, V_m, of 2.24×10^3 cm^3 mol^{-1} at stp, and with the regression line intercept c_3 used for log Y_Z. This leads to the equivalence

$$\lambda = 0.825(Y_Z)^{-1} \text{ nanometers} \qquad (52)$$

These values of λ so obtained are listed in Table VI and plotted as log λ for display against the transition-site aperture σ_L in Figures 8 and 9. With the exception of the PDMS (**E**) (where an unreasonably low value is obtained) and the three PEs (**E**, **G**, **H**) (where unreasonably high values are obtained), the remaining "core group" of 10 polymers gives an average value for λ of 10 nm. However, this average has an uncertainty (derived from the standard deviation of log λ) of a factor of 5 either way—that is, with λ ranging from 2 to 50 nm. The anomalous behavior of PDMS (**E**) and the three PEs (**F**, **G**, **H**) is discussed below (Anomalies in the Types 2, 3, and 4 Plots).

Table V Type 2 Plot—Parameters for the Linear Correlations Between Permeation Activation Energy E_P and Permeant Molecular Diameter σ_G

		Glass State: $T < T_g$			Rubber State: $T > T_g$		
#	Polymer	r_2	c_2	m_2	r_2	c_2	m_2
A	NR	?	?	?	0.311	*	*
B	PA	0.965	−106(27)	0.505(96)	0.965	−106(27)	0.50(10)
C	PC	0.969	−47(10)	0.24(3)	0.969	−180(35)	0.74(11)
D	PDMB	?	?	?	0.994	−130(11)	0.60(4)
E	PDMS	?	?	?	0.921	52(7)	−0.14(2)
F	PE1	?	?	?	0.965	−19(9)	0.18(3)
G	PE2	?	?	?	0.921	−24(14)	0.23(5)
H	PE3	?	?	?	0.943	−14(10)	0.19(3)
I	PETFE	0.084	*	*	0.084	*	*
J	PEMA	0.977	−60(10)	0.327(35)	0.977	−60(10)	0.33(4)
K	PET	0.946	−52(19)	0.275(66)	0.993	−145(16)	0.64(6)
L	PP	?	?	?	0.994	−29(5)	0.13(2)
M	PTFE	0.979	−59(10)	0.28(3)	0.979	−59(10)	0.28(3)
N	PVAC	0.857	−104(38)	0.43(13)	0.995	−206(11)	0.90(4)
O	PVBZ	0.956	−29(6)	0.17(2)	0.959	−68(13)	0.36(4)
P	PVC	0.889	−129(35)	0.60(12)	0.943	−265(50)	1.10(17)

See Table II for the polymer codes and details of the samples used. See Figure 6(A–P) for the respective plots. r_2, correlation coefficient; c_2, ordinate intercept—eq. (47); m_2, gradient—eq. (47). ?, no data available—sample not studied in this state; *, no meaningful data—poor linear correlation.

Type 4 Plot: Log Y Against Molecular Diameter σ_G

Background

This third type of test plot for the TSM theory looks for the correlations between the two parameters, log Y and the molecular diameter σ_G.

Results

The graphs for the 16 polymers are shown in Figure 10(A–P), with common scales for ease of comparison. In contrast to the Type 2 and Type 3 plots, these Type 4 plots give straight lines for all of the polymers, that is, now including NR (**A**) and PETFE (**I**), which gave scatters of points previously, and including the six "large" permeants—CO_2 (**j**), SO_2 (**k**), Cl_2 (**l**), SiF_4 (**n**), Xe (**o**), and SF_6 (**p**)—which showed consistent deviations in the previous two types of plot. As with the Type 2 plots, with the five polymers where the parameters are different for the glass and rubber states—PC (**C**), PET (**K**), PVAC (**N**), PVBZ (**O**), and PVC (**P**)—two straight lines of different slope are obtained.

The standard form of the regression equation here is

$$\log Y = m_4\sigma_G + c_4 \qquad (53)$$

The derived values of the linear regression parameters m_4 and c_4 are listed in Table VIII.

As with the previous two cases, the close fit to straight lines seen here even more generally gives us further confidence both in the values of the van der Waals molecular diameters for these molecules (Appendix B) and in literature data of the preexponential factor P_A (from which the value of the entropy function Y is obtained) for these systems.

Molecular Interpretation of the Type 4 Plots

Once again, the straight-line plots in Fig. 10 are consistent with a single type of transition site for each polymer. However, this evidently now includes the cases of NR (**A**) and PETFE (**I**) which did not show this behavior in the other plots, as well as the "large" permeants as listed above which generally showed deviant behavior with the two previous plots (Figures 4 and 6).

The straight lines evidently relate to a constant incremental effect of the permeant molecule diameter, σ_G, on the entropy of the surrounding matrix, S(L), since the translational entropy contribution of the permeant molecule has been eliminated by its insertion and entrapment in the aperture of the transition site. We may therefore

Table VI Transition-site Characteristics

		Glass State: $T < T_g$				Rubber State: $T > T_g$			
#	Polymer	σ_L	θ	log λ	ν	σ_L	θ	log λ	ν
A	NR	?	?	?	?	*	*	*	1.81(17)
B	PA	210(12)	0.84(16)	1.43(27)	2.83(24)	210(12)	0.84(16)	1.43(27)	2.83(24)
C	PC	196(15)	0.40(5)	0.85(107)	1.93(14)	243(12)	1.23(18)	0.85(107)	3.95(39)
D	PDMB	?	?	?	?	218(5)	0.99(6)	1.89(35)	4.49(17)
E	PDMS	?	?	?	?	369(11)	−0.23(4)	−5.00(31)	0.33(14)
F	PE1	?	?	?	?	101(29)	0.31(5)	9.09(160)	2.36(15)
G	PE2	?	?	?	?	105(35)	0.38(8)	7.99(293)	2.50(19)
H	PE3	?	?	?	?	76(35)	0.32(6)	13.00(210)	2.46(16)
I	PETFE	*	*	*	1.92(30)	*	*	*	1.92(30)
J	PEMA	184(11)	0.54(6)	1.39(166)	2.26(21)	184(11)	0.54(6)	1.84(166)	2.26(21)
K	PET	188(24)	0.46(11)	1.01(46)	1.90(28)	225(6)	1.07(9)	1.01(46)	4.01(42)
L	PP	?	?	?	?	216(8)	0.96(10)	2.42(78)	4.16(57)
M	PTFE	212(11)	0.46(6)	1.10(103)	2.21(33)	212(11)	0.46(6)	1.10(103)	2.21(33)
N	PVAC	239(11)	0.72(22)	0.52(24)	2.25(62)	230(3)	1.49(6)	0.52(24)	5.41(29)
O	PVBZ	176(14)	0.28(4)	0.39(54)	1.33(25)	188(12)	0.60(7)	0.13(54)	2.32(28)
P	PVC	216(13)	0.99(19)	0.15(30)	4.99(56)	241(7)	1.83(29)	0.15(30)	4.99(56)

See Table II for the polymer codes and details of the samples used. σ_L, transition-site aperture diameter (pm)—Figure 3; θ, force constant (nN)—eq. (48); λ, average transition-site spacing (nm)—Figure 3; ν, entropy increment (pJ K^{-1} m^{-1})—eq. (54). ?, no data available—sample not studied in this state. *, no meaningful data—poor linear correlation. See Figs. 8, 9, and 11.

define the *entropy increment* ν for this insertion process [eq.(19)] by

$$\nu \equiv \{\Delta S(\mathrm{GL})\}/\{\Delta\sigma_G\} \tag{54}$$

Combining this with eq. (42) gives

$$\nu = (R/\log e)\Delta\{\log Y\}/\Delta\sigma_G \tag{55}$$

and applying this to the regression expression eq. (53) gives

$$\nu = (R/\log e)m_4 \tag{56}$$

Since the entropy values S are in molar units, while the molecular diameters σ_G are in molecular units, it is again necessary to bring them into line by introducing the Avogadro number N_A, so that the conversion becomes first

$$\nu = (8.314/0.4343)m_4 \quad (\mathrm{J\ K^{-1}\ mol^{-1}})/(\mathrm{pm\ molecule^{-1}}) \tag{57}$$

which then gives

$$\nu = 31.8m_4 \qquad \mathrm{pJ\ K^{-1}\ m^{-1}} \tag{58}$$

where pJ is picojoules (10^{-12} J). The values of the entropy increment so-derived are listed in Table VI. They are also plotted against the values of the force constant θ in Figure 11. This shows a positive linear correlation between the plotted quantities for the 14 polymers [i.e., excepting NR (**A**) and PETFE (**I**)], but not a proportionality as might be expected; this correlation includes the three PEs (**F**, **G**, **H**) and PDMS (**E**) which are anomalous in their values of the transition-site aperture σ_L and the site-spacing λ (Figures 8 and 9).

It should be noted, in the molecular interpretation of these Type 4 plots, that the zero level of log Y has no fundamental significance because it can be shifted up or down by a change in the units of length or time. This contrasts with the status of the E_P values in the Type 2 plots (Fig. 6).

The curious feature of this Type 4 plot is that the linear plots (Fig. 10) now include the polymers NR (**A**) and PETFE (**I**) which previously gave "scattered" plots and, moreover, include the "large" permeants. It seems that although the two different groups of permeants ("small" and "large") may have to use two different sets of transition sites with different apertures, the entropy increment for the matrix surrounding them is still the same, giving the same slope for all permeants with a particular polymer.

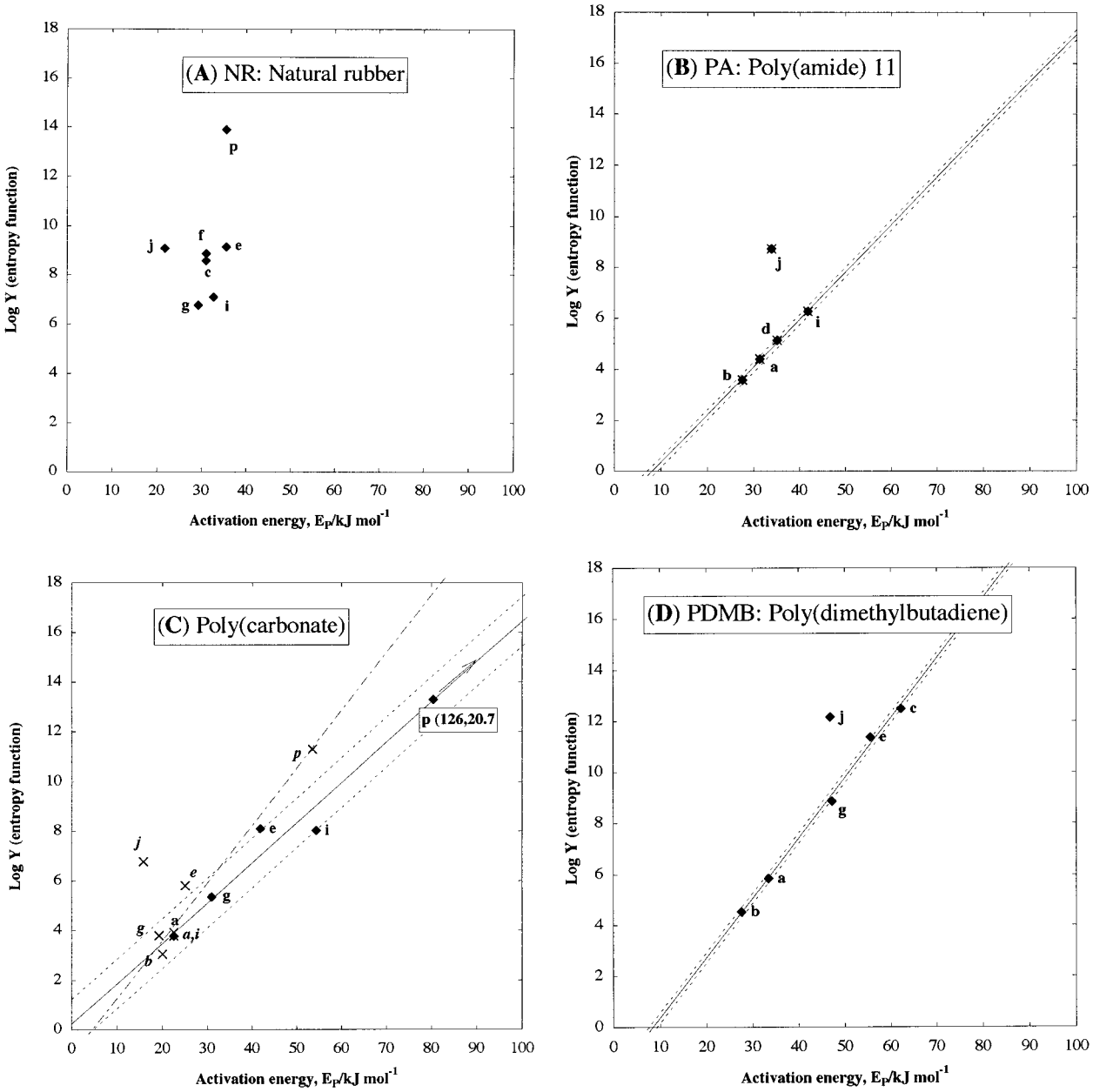

Figure 7 (A–P) Type 3 plots: log of the entropy function Y versus activation energy E_P; polymers, permeants, and symbols as Figures 4(A–P).

ANOMALIES IN THE TYPES 2, 3, AND 4 PLOTS

"Normal" Polymers and Permeants

Of the 16 polymers for which literature data were available (Table II), 10 of them showed consistent behavior in the three types of plots and gave consistent values of the four parameters derived (Table VI, and figs. 8, 9, and 11). Likewise, of the 16 permeants that had been studied with these polymers (Table III), the 10 "small" permeants showed consistent behavior. We may refer to these polymer/permeant pairs as the "core group" and as representing the "normal" behavior. We consider here the six polymers and the six per-

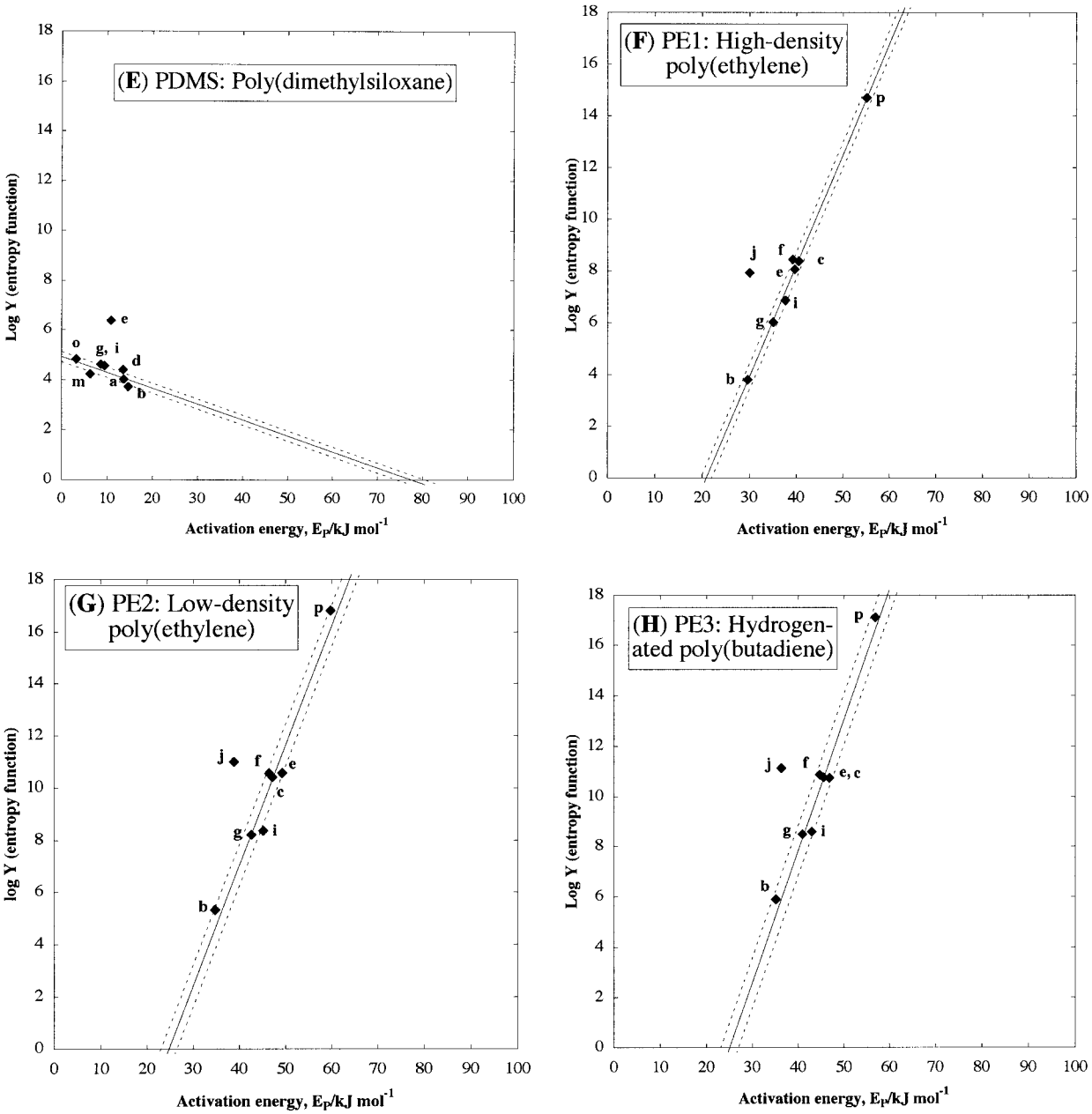

Figure 7 Type 3 plots (*Continued from the previous page*)

meants that showed anomalous behavior in one or more of these three types of plots.

NR (A)

This polymer showed only an apparent clustering in the Type 2 plot [Fig. 6(A)] and the Type 3 plot [Fig. 7(A)], but a linear correlation in the Type 4 plot [Fig. 10(A)]. This polymer differs from the others by being of natural origin. It may be speculated that there is a certain "copolymer" character for the polymer chain, which as seen with PETFE (**I**) leads to the same type of behavior in the plots. It also possible that the significant amounts of nonrubber contaminants (especially, proteins and fatty acids) in commercial samples of NR may play a part in this behavior. This evidently needs further examination in view of the importance of this polymer—specifically, by com-

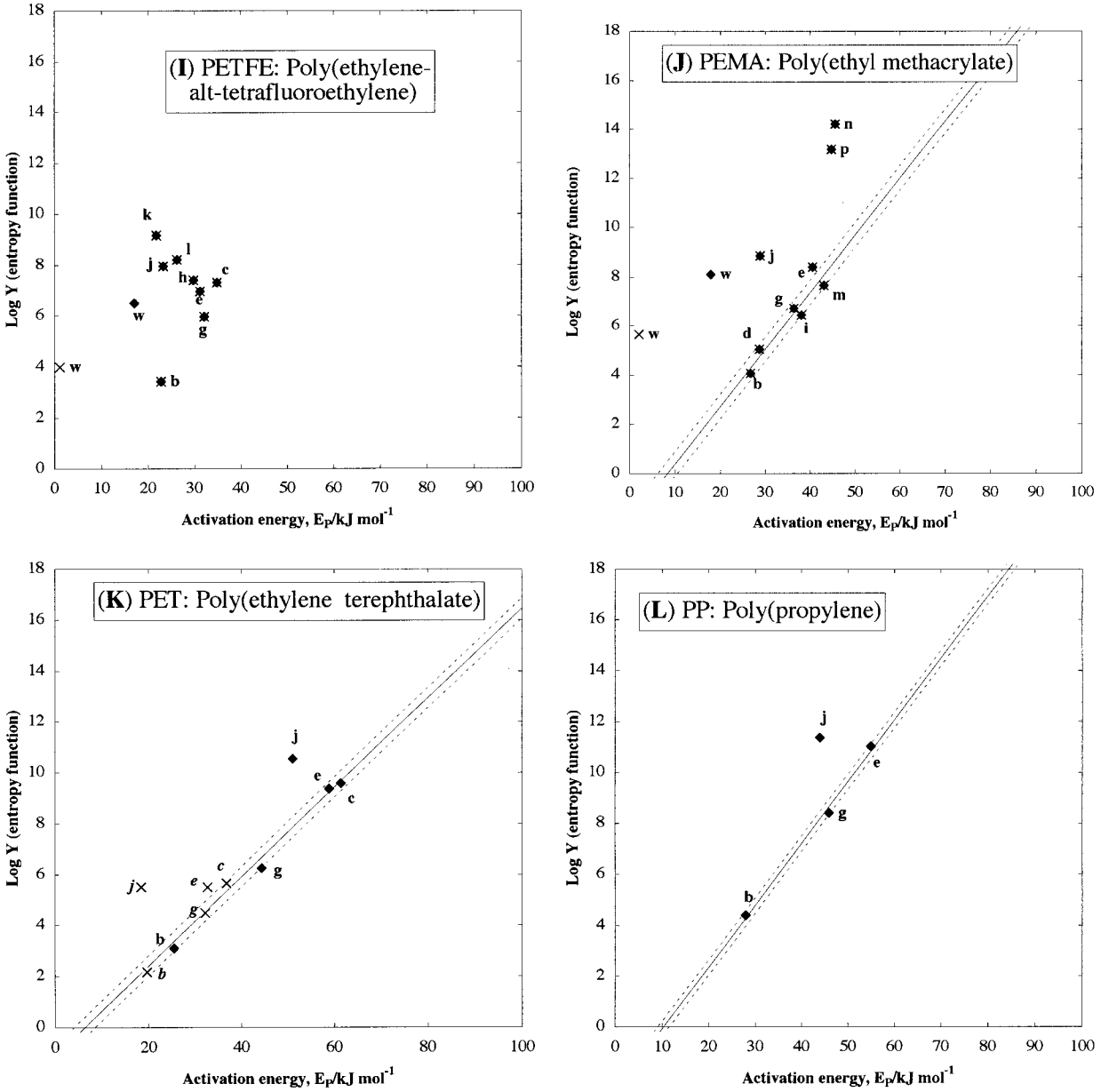

Figure 7 Type 3 plots (*Continued from the previous page*)

paring with the behavior of synthetic polyisoprenes and with that of NR that has been appropriately purified.

PDMS (E)

This polymer is anomalous in that it shows a negative slope in the Type 2 plot [Fig. 6(E)] and in the Type 3 plot [Fig. 7(E)], albeit with a positive (but rather small) slope in the Type 4 plot [Fig. 10(E)]. [In evaluating these three plots, it became evident that the data points for N_2 (**e**) are out of line. In particular, the log Y value is apparently 2 units too high, which may have arisen from the original value of P_A having been recorded too high by a factor of 100. The data for this permeant have therefore been omitted in processing the data for this polymer.] The Type 2 plot gave to a value of the transition-site aperture (369 pm) that is comparatively large but not unreasonable, but an apparently negative value for force constant θ; the Type 3 plot gave an unreasonably small value for the intersite spacing λ, while the Type 4 plot gave a value of the entropy increment ν that is

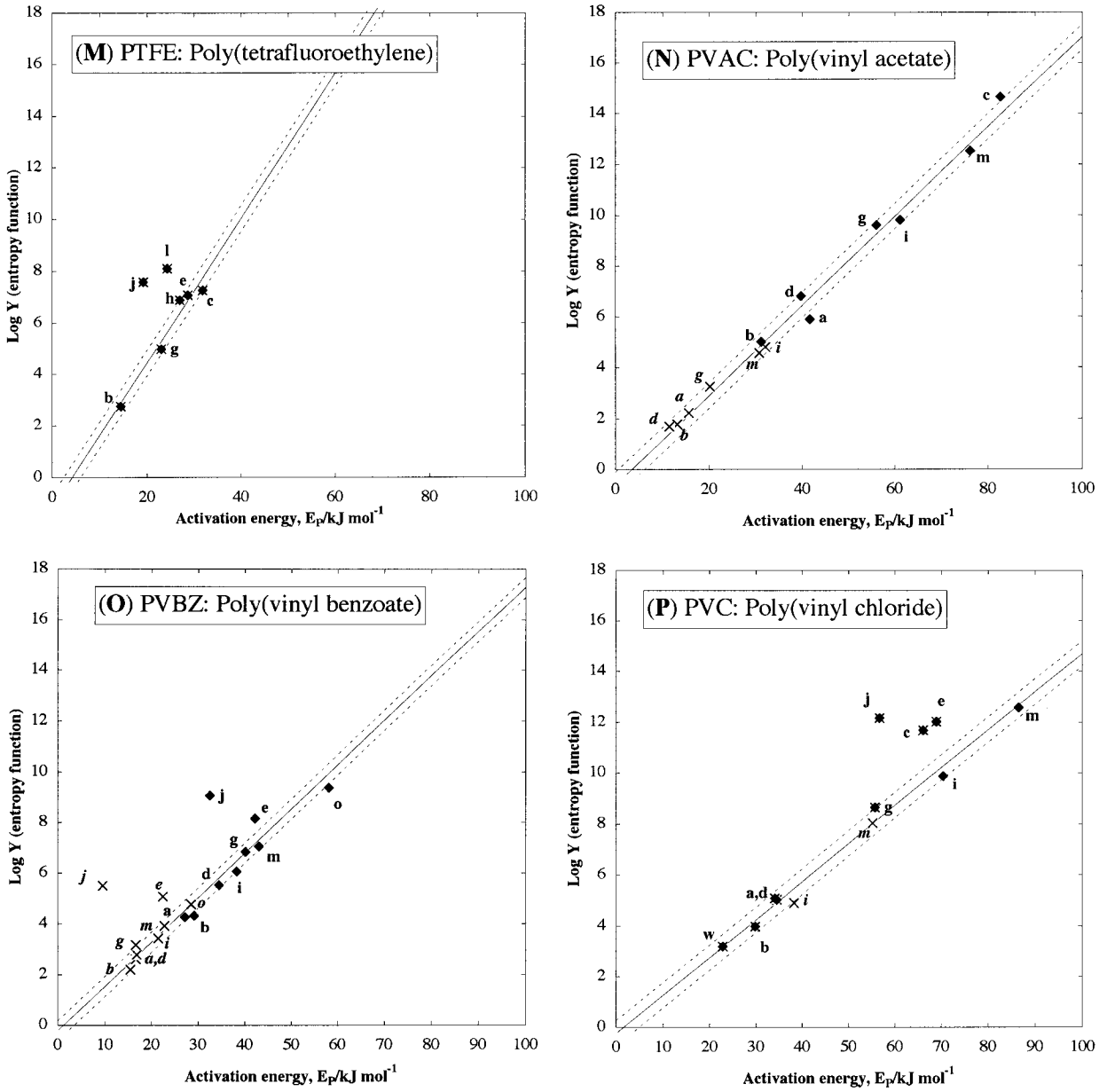

Figure 7 Type 3 plots (*Continued from previous page*)

relatively small although still positive (Table VI and figs. 8 and 11). From the molecular viewpoint, the difference between PDMS and the other polymers listed lies in the presence of the silicon atoms in the backbone. This leads to an unusually large flexibility of the chain and much easier segmental rotation.[59] This needs to be investigated by looking at the permeation behavior of other silicone-type polymers.

PE1 (F), PE2 (G), and PE3 (H)

These three polymers show essentially "normal" behavior in the Type 2 plots [Fig. 6(F–H)], the Type 3 plots [Fig. 7(F–H)], and the Type 4 plots [Fig. 10(F–H)]; the only anomaly here is that the data points for the "large" permeant SF_6 (**p**) lie close to the lines, whereas the other "large" permeant CO_2 (**j**) shows the same deviations seen in other cases. However, the derived values of the transition-site aperture σ_L are relatively small (average 96 pm), while the values of the site-spacing are impossibly large (Fig. 8). Nevertheless, the values of the thermodynamic properties θ and ν are in line with those of the other polymers (Fig. 11). It is difficult to see why this polymer, which is among the simplest structured of all

Table VII Type 3 Plot—Parameters for Linear Correlations Between log Y ("Entropy Function") and Permeation Activation Energy E_P

		Glass State: $T < T_g$			Rubber State: $T > T_g$		
#	Polymer	r_3	c_3	m_3	r_3	c_3	m_3
A	NR	?	?	?	0.695	*	*
B	PA	0.998	−1.51(27)	0.186(8)	0.998	−1.51(27)	0.186(8)
C	PC	0.981	−1.05(67)	0.232(23)	0.993	0.24(98)	0.162(14)
D	PDMB	?	?	?	0.999	−1.98(35)	0.235(7)
E	PDMS	?	?	?	0.744	4.92(31)	−0.063(28)
F	PE1	?	?	?	0.986	−9.17(160)	0.435(42)
G	PE2	?	?	?	0.959	−8.08(293)	0.383(65)
H	PE3	?	?	?	0.985	−13.0(210)	0.523(46)
I	PETFE	0.126	*	*	0.126	*	*
J	PEMA	0.946	−1.93(166)	0.232(46)	0.946	−1.93(166)	0.232(46)
K	PET	0.988	−1.10(46)	0.176(11)	0.988	−1.10(46)	0.176(11)
L	PP	?	?	?	0.997	−2.51(78)	0.243(18)
M	PTFE	0.981	−1.18(103)	0.281(39)	0.981	−1.18(103)	0.281(39)
N	PVAC	0.995	−0.61(24)	0.176(5)	0.995	−0.61(24)	0.176(5)
O	PVBZ	0.947	−0.21(54)	0.175(17)	0.947	−0.21(54)	0.175(17)
P	PVC	0.992	−0.23(30)	0.149(6)	0.992	−0.23(30)	0.149(6)

See Table II for the polymer codes and details of the samples used. See Figure 7(A–P) for the respective plots. r_3, correlation coefficient; c_3, ordinate intercept—eq. (49); m_3, gradient—eq. (49); ?, no data available—sample not studied in this state; *, no meaningful data—poor linear correlation.

polymers, should show these anomalies and that they occur even with some significant alterations to the polymer structure (in terms of the content of branches). By contrast, the closely related polyolefin polypropylene (**L**) falls within the normal "core group" in all its properties, although it does have a somewhat large value (260 nm) for the site-spacing λ (Table VI and fig. 9).

PETFE (I)

This polymer is somewhat similar in its behavior to NR (see above), showing only an apparent clustering in the Type 2 plot [Fig. 6(I)] and the Type 3 plot [Fig. 7(I)] but a linear correlation in the Type 4 plot [Fig. 10(I)]. It is possible that this anomalous behavior arises from the fact that the literature sample[6] was not a pure alternating copolymer as assumed.[60] For example, it may have an admixture with the homopolymers PE and PTFE. This would give a distribution of transition-site apertures and site-spacings, which would "cloud" the Type 2 and Type 3 plots; if, on the other hand, the entropy characteristics of the sites were similar, this could still give a linear Type 4 plot. The behavior of this copolymer evidently needs further study.

"Large" Permeants

These are the six permeants that have molecular diameters of 324 pm or greater (Table III), comprising CO_2 (**j**), SO_2 (**k**), Cl_2 (**l**), SiF_4 (**n**), Xe (**o**), and SF_6 (**p**). In the Type 2 plots, these show anomalously low E_P values [Fig. 6(B–D,F–H,J–M,O,P)], although the points for SF_6 (**p**) lie sometimes on or near the correlation line [Fig. 6(C,F)] and likewise for Xe (**o**) [Fig. 6(O)]. Similar behavior is seen in the Type 3 plots (Fig. 7); although this could be equally well interpreted as low log Y values, the fact that such anomalies are not seen in the Type 4 plots (Fig. 10) confirms that this corresponds to low values of the activation energy E_P.

From the molecular viewpoint, if we consider the type of transition site used by the "small" molecule permeants, it is evident that as the permeant molecular diameter is increased a certain critical size is reached at which the amount of energy required to insert the molecule becomes too great for insertion in the site to be feasible while still giving permeation at a detectable rate. The permeant molecules apparently are able to find a set of transition sites with a larger value for the aperture, giving a lower activation energy and, hence, a detectable rate of permeation. This

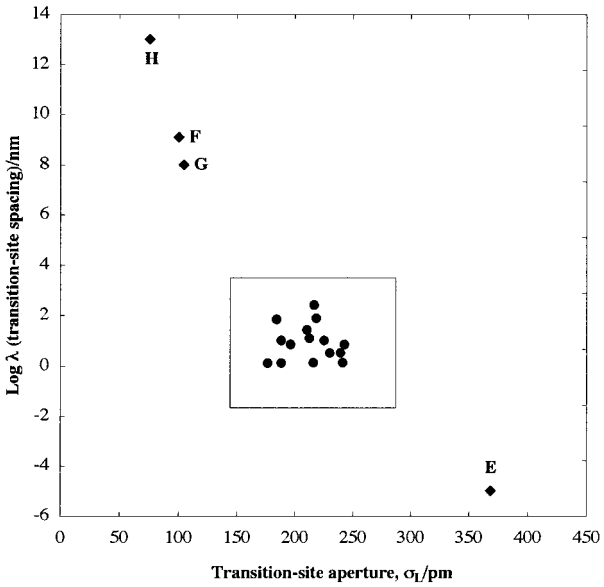

Figure 8 Transition-site characteristics: display plot of the log of the transition-site spacing λ (nm) versus the site aperture diameter σ_L (pm); polymers as listed in Table II; symbols as Figure 4(A–P); see Figure 9 for inset.

would correspond to correlation lines in the Type 2 plot (Fig. 6) shifted to higher σ_G values and, hence, to lower E_P values. However, there are not enough data on the "large" permeants in the present dataset to test this picture properly.

One of the curious common features in this respect is the sharpness of this transition, in that CH_4 (**c**), which has nominally the same molecular diameter σ_G (324 pm) as that of CO_2 (**j**), should apparently always behave as a "small" molecule and show "normal" behavior. The exception here is with PVC (**P**), where Figure 7(P), in particular, shows that not only CH_4 (**c**) but even N_2 (**e**) (σ_G = 313 pm) behave as "large" molecules with this polymer.

Water Vapor [H_2O (w)]

This is a very important permeant, which has, nevertheless, been treated apart from the others because its behavior is evidently distinct. The term "water vapor" is applied here to emphasize that it is the behavior of isolated water molecules that is involved, that is, the values of P are the ideal values P_I. We stay within the present dataset of polymer samples for comparison with the other permeants, since it is evident that (particularly with this permeant) the permeation behavior is sample-sensitive—thus, Barrie and Machin[28] obtained different values for the Arrhenius parameters for PEMA/H_2O from those (used here) obtained by Stannett and Williams.[29] This, unfortunately, reduces the polymer dataset to just three members: PETFE (**I**), PEMA (**J**), and PVC (**P**). Considering the effects of change of state (glass or rubber) with these polymers, with the first two, there are different values for the Arrhenius parameters in the two states (while the other permeants have the same values), whereas in the latter case, the Arrhenius parameters for H_2O are the same (while there are differences for the "large" permeants with this polymer).

One problem that arises with this permeant is uncertainty in the value of the molecular diameter, which the van der Waals data indicate to be 289 pm (Table III and Appendix B). Evidently, further work needs to be done with this permeant along with related permeants on the same polymer sample. For example, there is scope for the use of heavy water (D_2O) to see the effect of the different hydrogen isotope. Likewise, systematic studies on the same polymer sample with the isoelectronic series: Ne, HF, H_2O, NH_3, CH_4, may show up effects from hydrogen bonding at the transition site; in the absence of such effects,

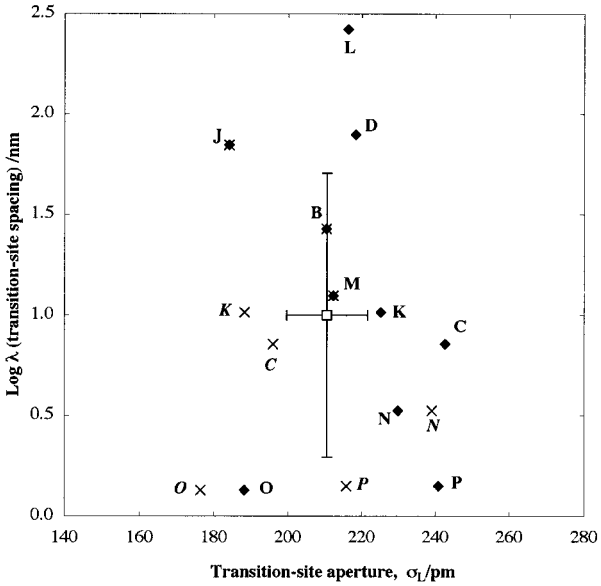

Figure 9 Transition-site characteristics: display plot of the log of the transition-site spacing λ (nm) versus the site aperture diameter σ_L (pm); polymers as listed in Table II (see also Fig. 8). (□) Mean point with mean standard deviation error bars; other symbols as Figure 4(A–P).

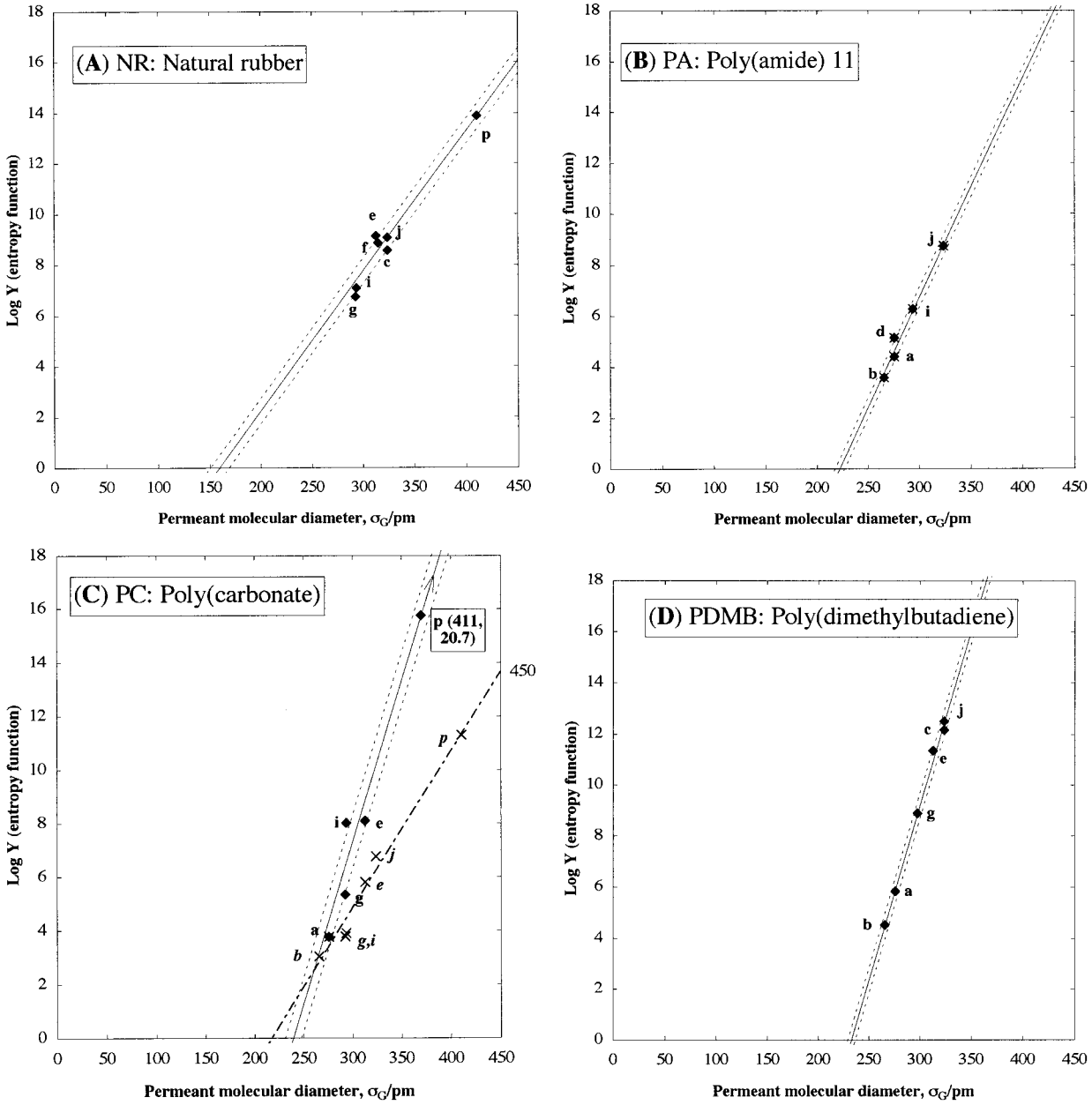

Figure 10 (A–P) Type 4 plots: log of the entropy function Y versus permeant molecular diameter σ_G; polymers, permeants, and symbols as in Figure 4(A–P).

there might be expected to be a smooth gradation of behavior along the series.

DISCUSSION

Predictive Character of the Theory

It should be recollected that the two main aims of any theory are to be (a) explanatory and (b) predictive. The explanatory aspect has been explored in the earlier interpretation of the test plots. From the predictive viewpoint, for a permeant not previously studied, given that its molecular diameter and absolute entropy are known, it should be possible to use the Types 2, 3, and 4 plots to interpolate the values of the Arrhenius parameters for permeation with the polymers listed here. More generally, it would be expected that other polymer/permeant systems would give the linear plots seen with the present systems; these would

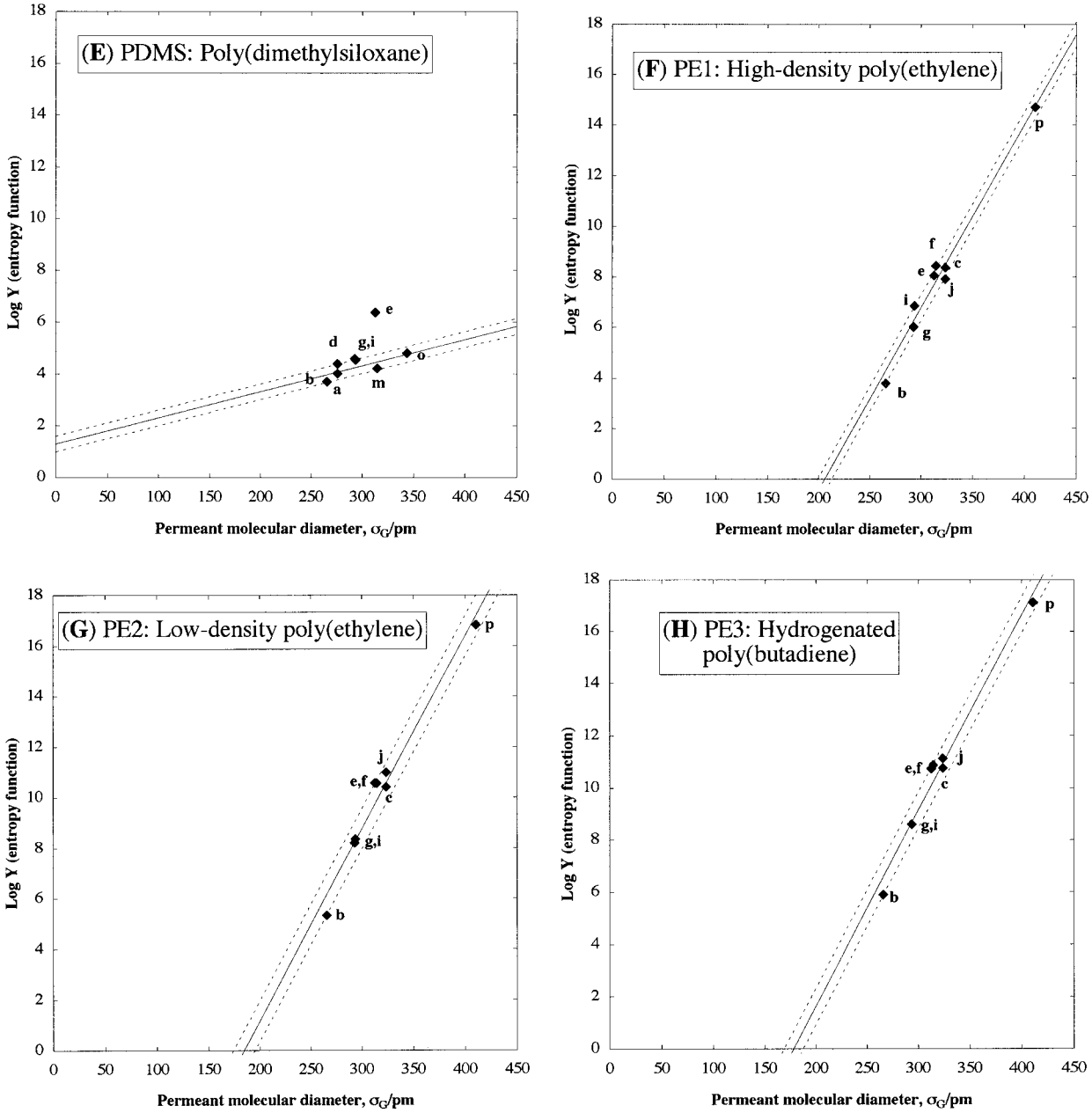

Figure 10 Type 4 plots (*Continued from the previous page*)

give the characteristic parameters derived here (Table VI). These parameters enable the permeability coefficient of the polymer/permeant pair at any temperature to be calculated. Ideally, these parameters should be related to known physical characteristics of the systems, that is, to the molecular and thermodynamic properties of the polymer and the permeant; as regards the polymer component, this last step does not seem to be feasible at the present stage, since the parameters do not seem to be related (for example) to the molecular structure of the chain unit (Table II).

Special Characteristics of the Transition Sites

There a number of special characteristics of the transition sites that have to be borne in mind in discussing the results obtained from the present treatment.

In the first place, we have the ironic situation that although the present materials are defined in the first instance to be nonporous (at least at the macroscopic level) the TSM theory leads logically to the revelation of the present transition sites as "porelike" features at least at the molec-

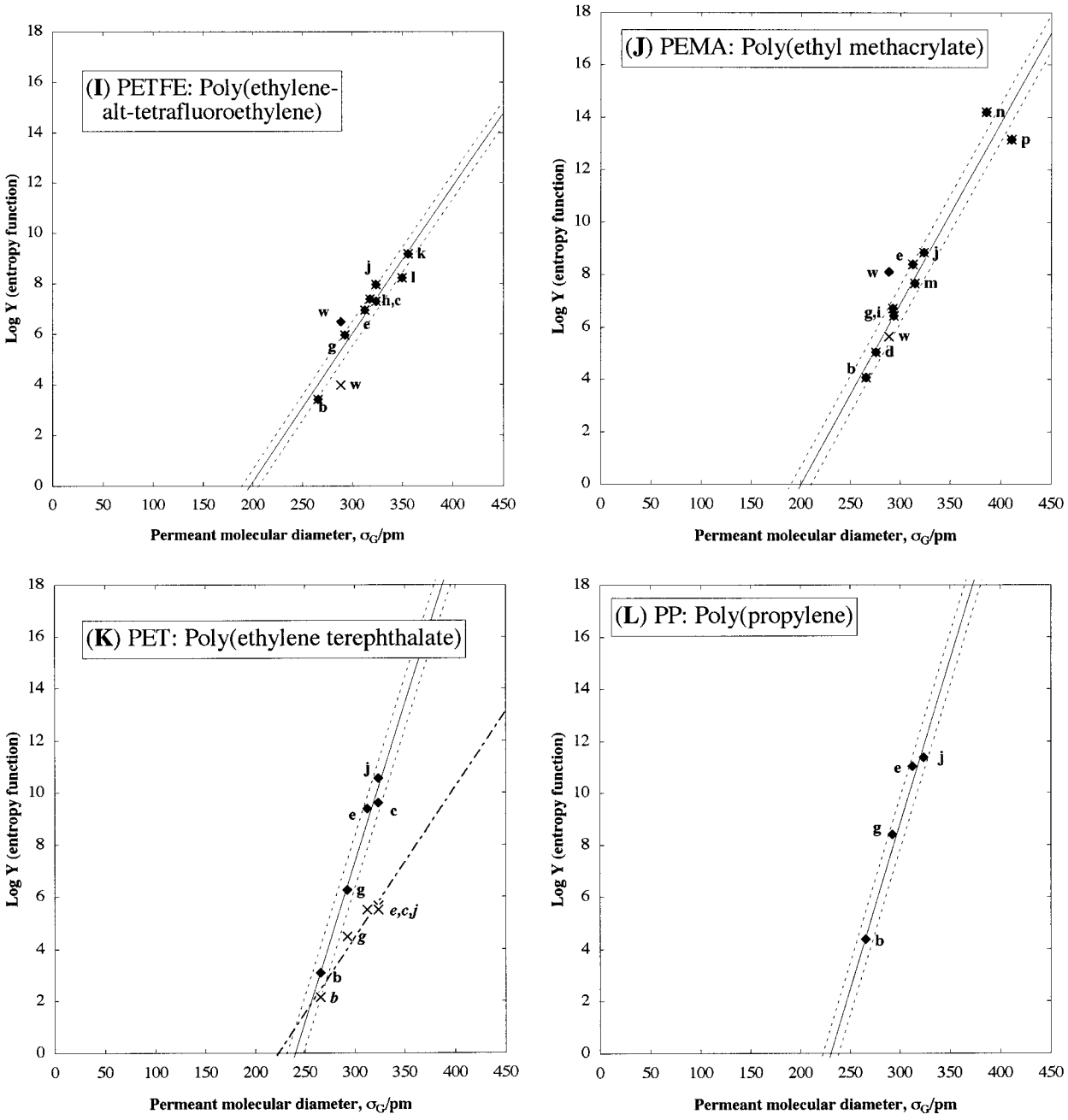

Figure 10 Type 4 plots (*Continued from the previous page*)

ular level. It would be useful to have a more descriptive name for these features. They were referred to as "bottlenecks" in an earlier and preliminary presentation of the theory,[25] but this does not really reflect the fact that they must be symmetrical in the forward and reverse direction, that is, along the x-axis as represented in Figure 3. In the behavior of crystalline solids, they are described as "saddle points," but, again, this does not reflect their three-dimensional character.[42] Possibly, the term "hourglass constriction" provides the best picture of their nature.

Second, these sites by definition are special features of the polymer, with characteristics that are not necessarily the same as those of the bulk polymer. In particular, the extensibility of the transition-site aperture should not be expected to relate to the Young's modulus of the bulk poly-

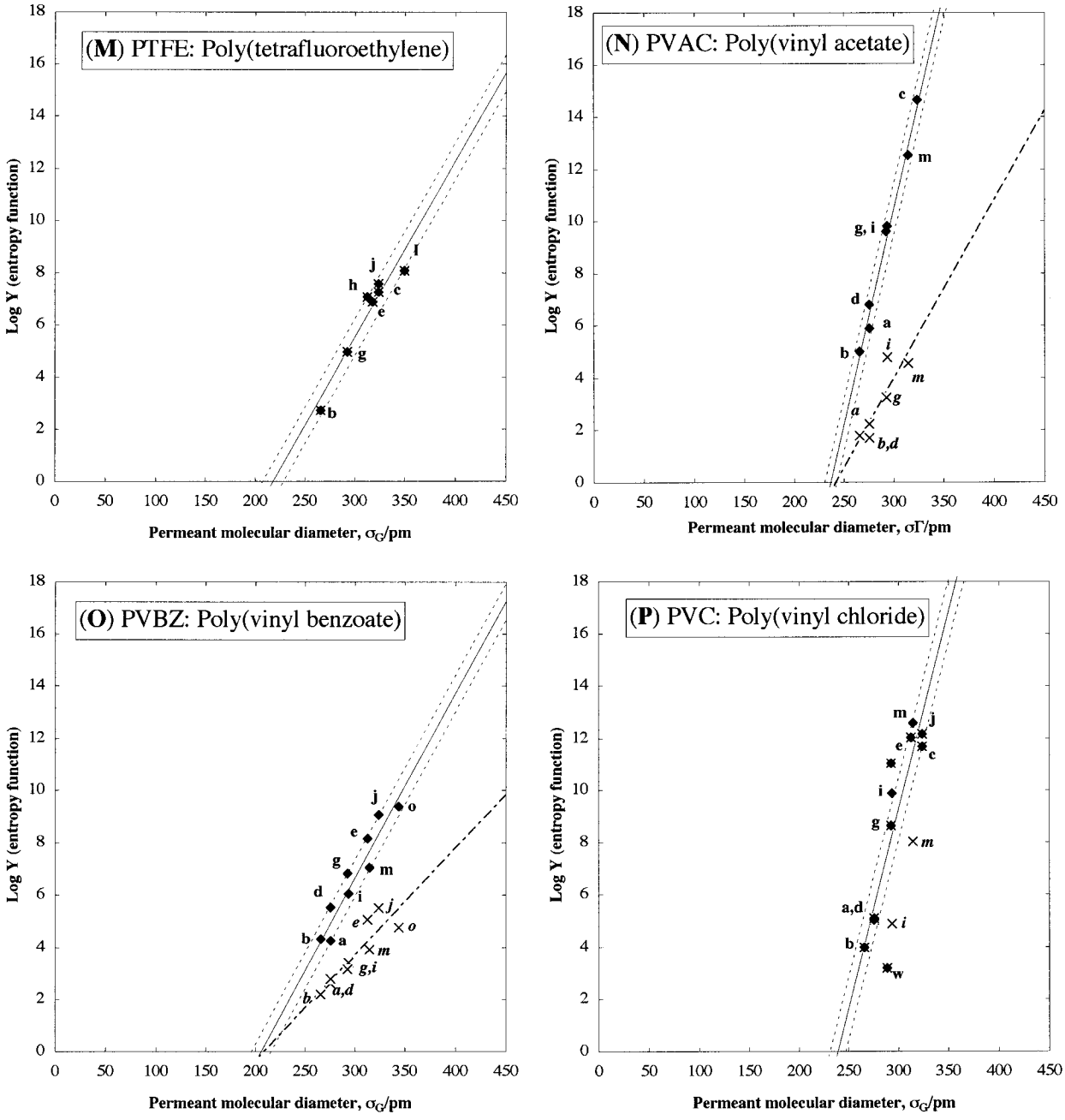

Figure 10 Type 4 plots (*Continued from the previous page*)

mer. This shows itself more fundamentally in the fact that this extensibility is defined by the force constant θ that is simply a force rather than the ratio force/distance. Curiously, this value of θ is lower for the glass state than for the rubber state, reflecting the relative activation energies (Table VI and Fig. 11); this is in contrast to the more extensible character of the polymer in the rubber state. However, this interpretation depends on the geometry of the interaction between the transition site and the permeant molecule, for the "extension" in question is not that of (say) a strip of the polymer, but rather of an hourglass-shaped hole into which the molecule is inserted. These remarks apply specifically to fully amorphous polymers; with semicrystalline polymers, they relate to the behavior of amorphous regions only, so that links between transition-site characteristics and those of the bulk polymer become more tenuous.

Table VIII Type 4 Plot—Parameters for the Linear Correlations Between log *Y* ("Entropy Function") and Permeant Molecular Diameter σ_G

		Glass State: $T < T_g$			Rubber State: $T > T_g$		
#	Polymer	r_4	c_4	m_4	r_4	c_4	m_4
A	NR	?	?	?	0.983	−8.8(17)	0.055(5)
B	PA	0.989	−19.2(21)	0.086(7)	0.989	−19.2(21)	0.086(7)
C	PC	0.987	−12.8(13)	0.059(4)	0.990	−28.8(39)	0.120(12)
D	PDMB	?	?	?	0.998	−31.9(16)	0.137(5)
E	PDMS	?	?	?	0.760	1.30(128)	0.010(4)
F	PE1	?	?	?	0.989	−14.9(15)	0.072(5)
G	PE2	?	?	?	0.985	−14.0(19)	0.076(6)
H	PE3	?	?	?	0.989	−13.4(16)	0.075(5)
I	PETFE	0.943	−11.5(30)	0.058(9)	0.943	−11.5(30)	0.058(9)
J	PEMA	0.975	−13.8(21)	0.069(6)	0.975	−13.8(21)	0.069(6)
K	PET	0.970	−13.0(26)	0.058(8)	0.989	−29.3(39)	0.122(13)
L	PP	?	?	?	0.991	−29.2(52)	0.127(17)
M	PTFE	0.957	−14.7(32)	0.067(10)	0.957	−14.7(32)	0.067(10)
N	PVAC	0.876	−16.6(54)	0.068(19)	0.994	−39.0(25)	0.165(9)
O	PVBZ	0.896	−8.5(23)	0.041(8)	0.959	−14.5(26)	0.071(8)
P	PVC	0.964	−36.4(50)	0.152(17)	0.964	−36.4(50)	0.152(17)

See Table II for details of the polymer codes and samples used. See Figure 10(A–P) for respective plots. r_4, correlation coefficient; c_4, ordinate intercept—eq. (53); m_4, gradient—eq. (53). ?, no data available—sample not studied in this state; *, no meaningful data—poor linear correlation.

Extension to Other Polymers

The present data taken from the *Polymer Handbook*, although extensive, evidently only represent a fraction of the data in the literature. For example, Lundstrom presented extensive data on a number of polymers—PEs, PTFE, NR, PDMS, and polymethylphenylsiloxane—with a range of permeants: noble gases (He, Ne, Ar, Xe, Kr), CO_2, CH_4, C_2H_6, and C_3H_8.[44,45] Likewise, Berens and Hopfenberg reported data for the two other important polymers, polystyrene and poly(methyl methacrylate), with a range of permeants and examined correlations with the permeant molecular diameter.[71] However, in both cases, the focus was placed entirely on the parameters for diffusion, to the exclusion of those for permeation, so that the data cannot be examined according to the present treatment; this is a common problem.

In the present literature data, emphasis has been placed on homopolymers. Copolymers have been extensively developed technically for their permeation properties; however, the present case of PETFE (**I**) suggests there may be problems in applying the present treatment because of the effect of a mixture of types of transition sites that may cloud the simple picture developed here. The same would apply also to homogeneous mixtures of polymers.

Extension to Other "Small" Permeants

Considering the scope for further work on this class of permeant, one problem to be tackled is the better definition of the regression lines from the three types of plots (Types 2, 3, and 4) so as to determine the transition-site characteristics more precisely (Figs. 6, 7, 10). At the lower end of the line, this would mean using isotopic species, that is, ^{3}He, HD, and D_2. These could be considered to be distinct molecular species from ^{4}He (the present He) and H_2 that presently define the lower end; they might, at the same time, show up isotope effects. For intermediate points, more work with permeants such as CO, NO, and F_2 would supplement the present data for N_2 and O_2. For the upper end, isotopically substituted CH_4 (i.e., CH_3D, CH_2D_2, CHD_3, and CD_4) could provide distinct molecular species to define this region of the plots more precisely. One general limitation would be the availability of the van der Waals diameters (Appendix B) and the absolute entropies (Appendix C) for the isotopically substituted molecules.

Extension to Other "Large" Permeants

The present systems show a more or less sharp distinction between the behavior of CH_4 (**c**) and

that of CO_2 (**j**), which, although having nominally the same molecular diameter (324 pm), fall into the "small" and "large" permeant classes, respectively. This transition could be explored using the analog N_2O (σ_G = 328 pm) and the larger noble gases: Ar (294 pm), Kr (315 pm), and Xe (344 pm).

In addition, there is ample scope for the study of the larger molecule permeants, in particular, to see whether the immediately larger ones define a correspondingly larger aperture transition site for the polymers in question—that is, give plots which linear but are shifted across to higher σ_G values.

With the larger-molecule permeants, two new features arise: In the first place, it introduces extended-molecule permeants such as the longer-chain alkanes, where the assumption of an effectively spherical shape for the permeant molecule no longer applies.

Furthermore, even with compact molecule organic substances, these are, generally, more strongly sorbed by the polymer, leading to "plasticization" effects. It is therefore essential that data be extrapolated to zero vapor pressure so that it is the ideal permeation coefficient that is involved. Likewise, with permeants that are liquid or solid in the pure state, the rate of permeation must be converted the standard units (Appendix A), taking into account the vapor pressure of the substance.

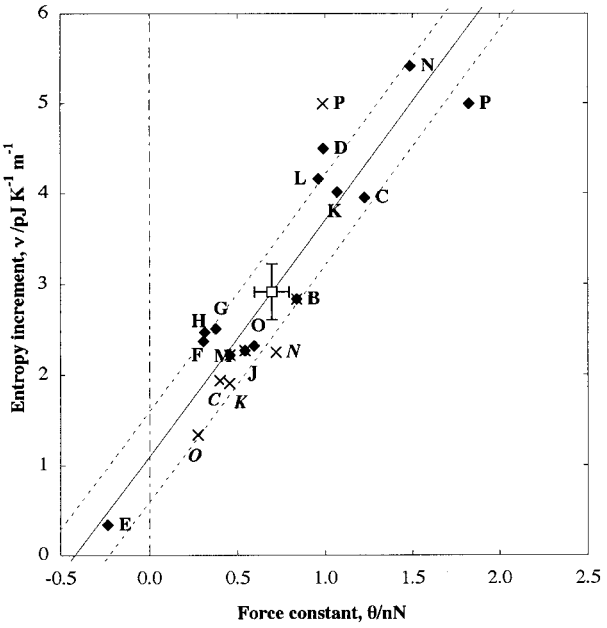

Figure 11 Transition-site characteristics: entropy increment ν (pJ K^{-1} m^{-1}) versus force constant θ (nN); polymers as listed in Table II. (□) Mean point with mean standard deviation error bars; other symbols as Figure 4(A–P).

CONCLUSIONS

- In the currently accepted conventional picture, the permeation of gases and vapors (permeants) through compact films of polymers is viewed as the consequence of the two fundamental processes: (a) the sorption equilibrium and (b) the kinetic process of diffusion. By contrast, in the theoretical picture presented here, permeation is considered as a fundamental process, with diffusion then viewed as a secondary process.
- In the present article, permeation is characterized at the molecular level by two processes: (a) the attachment (insertion) of the permeant gas molecule in the aperture of a transition site; and (b) its release therefrom according to transition-state theory.
- In this theory, the permeant molecules are taken to behave as "hard spheres," and their permeation behavior is taken to be little affected by their other chemical features.
- This picture has been justified from the literature data considered, at least for the "small" permeants (He to CH_4) and a "core group" of 10 polymers.
- The theory has led to the evaluation of quantities defining: the size of the transition-site aperture; the average spacing between these sites in the polymer; and the thermodynamic characteristics (energy and entropy changes) for the insertion process.
- Further work needs to be done to bring the "large" permeants (CO_2 and larger) into the same picture.
- The present theory provides a new basis for the rational interpretation and design of the permeation behavior of polymers.

NOMENCLATURE

A	area of permeation for the sample
AJM	activated-jump model for diffusion
A, . . . ,**V**	Stannett–Szwarc polymer dataset (Table I)
A, . . . ,**P**	present polymer dataset (Table II)
a, . . .,**p**	present permeant dataset (Table III)

b thickness of polymer sample (film, membrane, sheet, etc.)
B sorption coefficient—eq. (5)
B_I ideal sorption coefficient—eq. (6)
B_V sorption preexponential factor—van't Hoff eq. (11)
c concentration of permeant in the polymer
d depth of the permeation plane in the film—Figure 3
D diffusion coefficient—eq. (3)
D_A diffusion preexponential factor—Arrhenius eq. (10)
D_I ideal diffusion coefficient—eq. (4)
E_D diffusion activation energy—eq. (10)
E_P permeation activation energy—eq. (9)
G permeant gas (or vapor) molecule
GL permeant molecule inserted in the transition site—eq. (19)
h Planck constant (6.626×10^{-34} J s)
$K^{\ddagger}$ equilibrium constant for the insertion process—eq. (20)
$k^{\ddagger}$ rate constant for the release of G from GL—eq. (31)
L transition-site location—Figure 3
n number of occupied transition sites in the area exposed—eq. (22)
n_{tot} total number of transition sites in the area exposed—eq. (23)
N_A Avogadro constant (6.023×10^{23} molecules mol^{-1})
p vapor pressure of permeant gas G
P permeability coefficient—eq. (1) (see Appendix A for the "standard" units used here)
P_A permeation preexponential factor—Arrhenius eq. (9)
P_I ideal permeability coefficient—eq. (2)
PMR Principle of Microscopic Reversibility
q molecular rate of permeation from the occupied transition sites L
Q rate of permeation–eqs. (1) and (29)
R gas constant (8.314 J K^{-1} mol^{-1})
stp standard temperature (0°C = 273.2 K) and pressure (1 atm = 1.013×10^5 Pa)
S^0 absolute entropy—Appendix C
T absolute (thermodynamic) temperature (K)
T_g glass transition temperature (K) for the polymer
T_i isokinetic (isopermeation) temperature (K)—eq. (46)
TSM transition-site model for permeation
x axis of permeation—Figure 3
x general depth in polymer film ($0 \leq x \leq b$)—Figure 3
y, z axes perpendicular to direction of permeation—Figure 3

Greek Symbols

Δc concentration difference across the sample—Figure 3
$\Delta G^{\ddagger}$ standard free energy change for the insertion process—eq. (32)
ΔH_B standard enthalpy change for sorption—eq. (11)
$\Delta H^{\ddagger}$ standard enthalpy change for the insertion process—eq. (33)
$\Delta U^{\ddagger}$ standard internal energy change for the insertion process—eq. (34)
Δp pressure difference across the sample—Figure 3
$\Delta S^{\ddagger}$ standard entropy change for the insertion process—eq. (33)
θ transition-site force constant—eq. (48) and Table VI
λ average spacing between neighbor transition sites (lattice spacing for cubic model of TSM, jump distance in AJM)—Figure 3 and Table VI
ν transition-site entropy increment—eq. (54) and Table VI
ϕ_a volume fraction amorphous content of the polymer sample
ρ polymer density
σ_G permeant molecular diameter—Table III and Appendix B
σ_L diameter of the unoccupied transition-site aperture—Figure 3 and Table VI
π_S Salame permeation "Permachor"—eq. (15)

Superscripts

‡ transition state or transition site

Other Symbols

<Pa> "hidden" logarithmic units in absolute entropy values—Appendix C

Presentation of Statistical Results

Statistical results from sets of data are presented in the format: "mean(standard deviation)," with

the standard deviation value referred to the last significant figure quoted for the mean value. For example, "1.23(45)" represents a mean value of 1.23 with a standard deviation of 0.45.

APPENDIX A: UNITS FOR THE PERMEABILITY COEFFICIENT

A wide variety of units have been used for the permeability coefficient P. With gaseous (vapor) permeants, this results at least, in part, from it being derived as the quotient:

(amount of permeant × film thickness)
÷ (film area × time interval
× pressure difference across the film)

with a variety of forms for each these five quantities depending on the application [Eq. (1)]. The commonly used forms of unit and their interconversion factors have been tabulated and discussed.[6,7,72]

In the present article, with gaseous (vapor) permeants, values of P have been put into the "standard" units that are used in the *Polymer Handbook*[6]:

$$\text{cm}^3(\text{stp})\ \text{cm}/\text{cm}^2\ \text{s Pa}$$

where "stp" denotes that the volume of gas has been converted to standard temperature (0°C = 273.2 K) and standard pressure (1 atm = 1.013×10^5 Pa), and Pa denotes the pascal as the SI unit of pressure.

In the cases of liquid or solid permeants, the amount is generally put in terms of the mass penetrating, and any pressure units are omitted. Values of P calculated on such a basis need to be converted to the above form, for comparison with gas permeation data, taking into account the vapor pressure of the permeant.

Even the above "standard" units are evidently not in full accord with the SI system, since the amount should be put in moles and the dimensions should be in meters rather than centimeters; this is the basis used, for example, in the parallel area of permeation though inorganic membranes.[73] To take this a stage further, it would be more rational to replace the gas pressure by its volume (molar) concentration in the gas phase, since it is this concentration rather than any mechanical effect of the gas (from its static pressure) that is the controlling factor.

APPENDIX B: MOLECULAR DIAMETERS OF THE PERMEANT GASES

Sources of Data

In considering the values of molecular diameter to be used, the problem arises that it is difficult to find a consistent set of these values. For example, it might be expected that the diameters would be best defined for the noble gases, since they are monatomic. Lundstrom[45] reviewed the literature for these substances in the polymer/gas diffusion context. However, in the case of argon, he found that there were eight different values reported which ranged from 300 pm (3.00 Å) to 404 pm (4.04 Å), that is, an overall spread of about 30%. This uncertainty becomes more serious when correlations are sought with the square or the cube of the value.

In the present case, the values used have been based upon the literature data of the covolume, b, in the van der Waals equation of state for the gas, since these are tabulated for a wide range of gases and vapors.[74] Parallel data are also available for molecular dimensions derived from the gas viscosity, using the Lennard-Jones equation of state; this gives somewhat different numerical values, which may, nevertheless, be used for comparative and checking purposes.[75]

This van der Waals covolume b represents the volume that the molecule in the dilute gas excludes toward other molecules of the same kind; it may be equated to four times the volume of the molecule itself.[76] The molecular diameter σ_G will then be given by

$$\sigma_G = (3b/2\pi N_A)^{1/3} \qquad \text{(B.1)}$$

where N_A is the Avogadro constant, required to convert from a molar to a molecular basis. The literature values of b for the present permeant gases[74] together with the values of σ_G derived using eq. (B.1) are listed for the permeant dataset in Table III. There are two points that arise in connection with this listing:

Neon [Ne (e)]

The literature value of the van der Waals covolume b (in $\text{cm}^3\ \text{mol}^{-1}$) for this gas is 16.72, which

is lower even than that for H_2(**a**) (26.51) or He (**b**) (23.80).[74] Furthermore, a plot (not shown) of b versus the atomic number (i.e., electronic number) for the noble gases is essentially linear, but the point for Ne lies well below the line through the other gases; the interpolated value of b for Ne from this line is about 27.6. The viscosity/Lennard-Jones value of σ_G for Ne is also higher and close to that for H_2.[75] For these reasons, in the present case, the value of the molecular diameter σ_G for Ne has been taken to be the same as that for H_2, that is, 276 pm (Table III). This is in accord with the fact that the Arrhenius parameters for permeation with these two gases are also generally similar.

Water Vapor [H_2O (w)]

The van der Waals covolume b (in $cm^3\ mol^{-1}$) for this vapor is compared with the values for other members of the series of isoelectronic molecules containing this molecule: Ne, 26.51 (see above); HF 73.90; H_2O, 30.49; NH_3, 37.13; CH_4, 43.01.[74] Even disregarding the evidently anomalous value for HF, the value for H_2O therefore seems to be rather small, if we assume a monotonic (possibly linear) dependence of b for these molecules on the hydrogen number. However, there are uncertainties with the three molecules HF, H_2O, and NH_3 about the extent of hydrogen bonding between these molecules in the gas state and whether this has been "extrapolated out" by considering sufficiently low pressures; such association may be responsible for the high value for HF listed above. These uncertainties should be borne in mind in using the derived value of σ_G (289 pm) for H_2O as listed in Table III.

Validity of the σ_G Values from the Permeation Data

These values of the molecular diameter are evidently important in applying the present TSM. However, the literature values have a certain degree of suspicion attached to them; this arises, in part, from the approximate character of the van der Waals equation itself and, in part, from difficulties in the concept of a "hard-sphere" diameter for a molecule.

It is possible to obtain some idea of the validity of the σ_G values from the permeation graphs, particularly the Type 2 plots [Fig. 6(A–P)] and the Type 4 plots [Fig. 10(A–P)] which involve these values. Any scatter in these plots results from uncertainties in both σ_G and the other plotted quantity (E_P in the first case, log Y in the second). It is therefore remarkable that in many cases the plots are so close to linear. Unless this linearity is coincidental, then even disregarding any scatter due to the other plotted quantity, this indicates that the σ_G values are, in general, uncertain to only about 2 pm; this only applies to the "small" permeants in the first case, but includes some of the "large" ones in the second case. It is intriguing that it is apparently possible to validate such basic physicochemical data as molecular diameters from the study of permeation through films of polymers.

APPENDIX C: ABSOLUTE ENTROPIES OF THE PERMEANT GASES

Sources of Data

The absolute entropy of a substance S^0 is a well-defined quantity whose value is available for a wide range of substances.[77,78] The term "absolute" relates to the reference to a temperature of zero degrees absolute as the state for which (with a few exceptions) the pure crystalline substance form has zero absolute entropy. It is used in the present case to convert the Arrhenius preexponential factor P_A to the newly introduced "entropy factor" Y as defined by eq. (41) and used in Type 3 and Type 4 plots. The S^0 values for the present permeant dataset are listed in Table III. There are two points that arise in connection with this listing:

Hidden Pressure Units

Caution is required in using these data in the present context, because of the presence of "hidden" logarithmic units of pressure, which are additive rather than the more common multiplicative form.[79] In particular, the tabulated values[77,78] relate to a standard state involving a pressure of 1 bar (i.e., 1×10^5 pascals) as the reference state; this replaces the atmosphere (1 atm = 1.013×10^5 pascals) previously used. Thus, the data in the literature for hydrogen[77] may be represented more completely by

$$S^0(H_2) = 131\ J\ K^{-1}\ mol^{-1}\ \langle bar \rangle \qquad (C.1)$$

where the term "⟨bar⟩" denotes these "hidden" pressure units.[79] However, in the present "stan-

dard" units for permeability coefficient (Appendix B), the pressure unit is the pascal (Pa), which will be carried over into to the derived preexponential factor P_A from eq. (9). To make these suitable for the calculation of the entropy function Y through its definition in eq. (41), the values have, therefore, to be adjusted by adding the "correction factor" of $R \ln (1 \times 10^5)$, that is, 96 J K^{-1} mol^{-1} ⟨Pa bar^{-1}⟩, giving in this case

$$S^0(H_2) = 227 \text{ J K}^{-1} \text{ mol}^{-1} \langle \text{Pa} \rangle \qquad (C.2)$$

The values in these units derived in this way are listed in Table III.

Oxygen [O_2 (g)]

In the present application, these values are used to derive the entropy function Y from the Arrhenius preexponential factor P_A. For most of the "small" permeants, the Type 3 and Type 4 plots (Figs. 7 and 10) gave well-defined linear regressions. However, even in these cases, the log Y data for O_2 (**g**) were systematically high when the literature value of 302 J K^{-1} mol^{-1} ⟨Pa⟩ for S^0 was used. Correlation of the other plotted quantity (E_P or σ_G) with the least-squares regression data gave an essentially constant "effective" value for S^0 of 256(5) J K^{-1} mol^{-1} ⟨Pa⟩. Any uncertainty in this value will be due, in part, to the experimental uncertainties in the literature values of the preexponential factor P_A used in calculating the entropy function Y. It was also notable that the Type 2 plots [E_P against σ_G—Fig. 6(A–P)] showed no such consistent deviations in the data for O_2 (**g**) for either coordinate. For these reasons, this value S^0 (O_2) = 256 J K^{-1} mol^{-1} ⟨Pa⟩ is listed in Table III as the "effective" value for permeation and used in the Type 3 and Type 4 plots.

REFERENCES

1. Meares, P. Polymers: Structure and Bulk Properties; Van Nostrand: London, 1965; pp 313–346.
2. Diffusion in Polymers; Crank, J.; Park, G. S., Eds.; Academic: New York, 1968.
3. Permeability of Plastic Films and Coatings to Gases, Vapors, and Liquids; Hopfenberg, H. B., Ed.; Plenum: New York, 1974.
4. Perry, R. H.; Green, D. W.; Maloney, J. O. Perry's Chemical Engineers' Handbook, 6th ed.; McGraw-Hill: New York, 1984; pp 17.14–17.34.
5. Polymer Permeability; Comyn, J., Ed.; Elsevier: London, 1985.
6. Pauly, S. In Polymer Handbook, 3rd ed.; Brandrup, J.; Immergut, E. H., Eds.; Wiley: New York, 1989; pp VI/435–VI/449.
7. Permeability and Other Film Properties of Plastics and Elastomers; Plastics Design Library: Norwich, NY, 1995.
8. Brydson, J. A. Plastics Materials, 6th ed.; Butterworth: London, 1995; pp 96–99.
9. Fick, A. Ann Phys Lpz 1855, 170, 59.
10. Graham, T. Philos Mag 1866, 32, 401.
11. Von Wroblewski, S. Wied Ann Phys 1879, 8, 29.
12. Daynes, H. A. Proc R Soc Ser A 1920, 97, 286.
13. Barrer, R. M. Diffusion In and Through Solids; Cambridge University: Cambridge, 1941.
14. Barrer, R. M. J Phys Chem 1957, 61, 178.
15. Doty, P. M.; Aiken, W. H.; Mark, H. Ind Eng Chem Anal Ed 1944, 16, 686.
16. Doty, P. J Chem Phys 1946, 14, 244.
17. Doty, P. M.; Aiken, W. H.; Mark, H. Ind Eng Chem 1946, 38, 788.
18. Stannett, V.; Szwarc, M. J Polym Sci 1955, 16, 89.
19. Rogers, C.; Meyer, J. A.; Stannett, V.; Szwarc, M. Tappi 1956, 39, 741.
20. Salame, M. SPE Trans 1961, 1, 153.
21. Salame, M.; Pinsky. J. J Mod Packag 1962, 36, 153.
22. Salame, M. Am Chem Soc Polym Prepr 1967, 8, 137.
23. Salame, M. J Polym Sci Polym Symp 1973, 41, 1.
24. Barrie, J. A. In Diffusion in Polymers; Crank, J.; Park, G. S., Eds.: Academic: New York, 1968; Chapter 8.
25. Molyneux, P. In Water: A Comprehensive Treatise; Franks, F., Ed.; Plenum: New York, 1975; Vol 4, pp 714–721.
26. Barrie, J. A.; Machin, D. J Macromol Sci-Phys B 1969, 3, 645.
27. Barrie, J. A.; Machin, D. J Macromol Sci-Phys B 1969, 3, 673.
28. Barrie, J. A.; Machin, D. Trans Faraday Soc 1971, 67, 244.
29. Stannett, V.; Williams, J. L. J Polym Sci Part C 1965, 3, 45.
30. Barrie, J. A.; Machin, D.; Nunn, A. Polymer 1975, 16, 811.
31. McCall, D. W.; Douglass, D. C.; Blyler, L. L.; Johnson, G. E. Macromolecules 1984, 17, 1644.
32. Rouse, P. E. J Am Chem Soc 1947, 69, 1068.
33. Hauser, P. M.; McLaren, A. D. Ind Eng Chem 1948, 40, 112.
34. Myers, A. W.; Meyer, J. A.; Rogers, C. E.; Stannett, V. Tappi 1961, 44, 58.
35. Barrer, R. M.; Barrie, J. A. J Polym Sci 1958, 28, 377.
36. Wellons, J.; Stannett, V. J Polym Sci Part A-1 1966, 4, 593.
37. Yasuda, H.; Stannett, V. J Polym Sci 1962, 57, 907.
38. Williams, J.L.; Hopfenberg, H.B.; Stannett, V. J Macromol Sci-Phys B 1969, 3, 711.

39. Brandt, W. W. J Phys Chem 1959, 63, 1080.
40. Frisch, H. L. Polym Lett 1965, 3, 13.
41. Jagodic, F.; Borstnik, B.; Azman, A. Makromol Chem 1973, 173, 221.
42. Lawson, A. W. J Phys Chem Solids 1957, 3, 250.
43. Lawson, A. W. J Chem Phys 1960, 32, 131.
44. Lundstrom, J. E. PhD Thesis; University of Kansas: Kansas City, 1970.
45. Lundstrom, J. E. Trans NY Acad Sci 1973, 35, 95.
46. Pace, R. J.; Datyner, A. J Polym Sci Polym Phys Ed 1979, 17, 437.
47. Pace, R. J.; Datyner, A. J Polym Sci Polym Phys Ed 1979, 17, 453.
48. Pace, R. J.; Datyner, A. J Polym Sci Polym Phys Ed 1979, 17, 465.
49. Denbigh, K. G. The Thermodynamics of the Steady State; Methuen: London, 1951.
50. Glasstone, S.; Laidler, K. J.; Eyring, H. The Theory of Rate Processes: The Kinetics of Chemical Reactions, Viscosity, Diffusion and Electrochemical Phenomena; McGraw-Hill: New York, 1941.
51. Glasstone, S. Textbook of Physical Chemistry, 2nd ed.; Macmillan: London, 1951; pp 1087–1111.
52. Kuppers, J. R.; Reid, C. E. J Appl Polym Sci 1960, 4, 124.
53. Reiss, H. J Chem Phys 1964, 40, 1783.
54. Peyser, P. In Polymer Handbook, 3rd ed.; Brandrup, J.; Immergut, E. H., Eds.; Wiley: New York, 1989; pp VI/209–VI/277.
55. Michaels, A. S.; Bixler, H. J. J Polym Sci 1961, 50, 393.
56. Michaels, A. S.; Bixler, H. J. J Polym Sci 1961, 50, 413.
57. Ash, R.; Barrer, R. M.; Palmer, D. G. Polymer 1970, 11, 421.
58. Norton, F. J. J Appl Polym Sci 1963, 7, 1649.
59. Barrer, R. M.; Chio, H. T. J Polym Sci Part C 1965, 10, 111.
60. Sperati, C. A. In Polymer Handbook, 3rd ed.; Brandrup, J.; Immergut, E. H., Eds.; Wiley: New York, 1989; pp V/48–V/51.
61. Michaels, A. S.; Vieth, W. R.; Barrie, J. A. J Appl Phys 1963, 34, 1.
62. Michaels, A. S.; Vieth, W. R.; Barrie, J. A. J Appl Phys 1963, 34, 13.
63. Sezi, R.; Springer, J. Colloid Polym Sci 1981, 259, 1170.
64. Sperati, C. A. In Polymer Handbook; 3rd ed.; Brandrup, J.; Immergut, E. H., Eds.; Wiley: New York, 1989; pp V/35–V/44.
65. Meares, P. J Am Chem Soc 1954, 76, 3415.
66. Meares, P. Trans Faraday Soc 1957, 53, 101.
67. Hirose, T.; Mizoguchi, K.; Kamiya, Y. J Appl Polym Sci 1985, 30, 401.
68. Tikhomirov, B. P.; Hopfenberg, H. B.; Stannett, V.; Williams, J. L. Makromol Chem 1968, 118, 177.
69. Barrer, R. M. In Diffusion in Polymers; Crank, J.; Park, G. S., Eds.; Academic: London, 1968; pp 165–217.
70. Aylward, G. H.; Findlay, T. J. V. SI Chemical Data, 2nd ed.; Wiley: Sydney, 1974; pp 98–99.
71. Berens, A. R.; Hopfenberg, H. B. J Membr Sci 1982, 10, 283.
72. Huglin, M. B.; Zakaria, M. B. Angew Makromol Chem 1983, 117, 1.
73. De Vos, R. M.; Verweij, H. Science 1998, 279, 1710.
74. CRC Handbook of Chemistry and Physics, 77th ed.; Lide, D. R.; Frederikse, H. P. R., Eds.; CRC: Boca Raton, FL, 1996–1997; pp 6.47–6.51.
75. Reid, R. C.; Prausnitz, J. M.; Poling, B. E. The Properties of Gases and Liquids, 4th ed.; McGraw-Hill: New York, 1987; pp 733–734.
76. Glasstone, S. Textbook of Physical Chemistry, 2nd ed.; Macmillan: London, 1951; p 294.
77. CRC Handbook of Chemistry and Physics, 77th ed.; Lide, D. R.; Frederikse, H. P. R., Eds.; CRC: Boca Raton, FL, 1996–1997; pp 5.1–5.3.
78. CRC Handbook of Chemistry and Physics, 77th ed.; Lide, D. R.; Frederikse, H. P. R., Eds.; CRC: Boca Raton, FL, 1996–1997; pp 5.4–5.60.
79. Molyneux, P. J Chem Ed 1991, 68, 467.